UNIVERSITY OF CAPE COAST

DYNAMIC ANALYSIS OF THE WEST AFRICAN MONSOON AND ITS VARIABILITY OVER GHANA

BY

FRANCIS NKRUMAH

Thesis submitted to the Department of Physics of the School of Physical Sciences, College of Agriculture and Natural Sciences, University of Cape Coast, in partial fulfillment of the requirements for the award of Master of Philosophy Degree in Physics

JUNE, 2014

DECLARATION

Candidate's Declaration

I hereby declare that this thesis is the result of my own original work and that no part of it has been presented for another degree in this University or elsewhere. Published quotations from other sources have been duly acknowledged.

Candidate's Signature:…….. Date:…….……

Name: Francis Nkrumah

Supervisors' Declaration

We hereby declare that the preparation and presentation of this thesis were supervised in accordance with the guidelines on supervision of thesis laid down by the University of Cape Coast.

Principal Supervisor's Signature:…… Date:……..….

Name: Dr. Nana Ama Browne Klutse

Co-Supervisor's Signature: …… Date:…….....

Name: Mr. David C. Adukpo

ABSTRACT

In this study, the International Center for Theoretical Physics' Regional Climate Model Version 4 (RegCM4) is used over the period 1998-2010, to study the dynamics of rainfall over West Africa. The study also attempts to understand the West African Monsoon (WAM) circulation and its characteristics. Global Precipitation Climatology Project precipitation (GPCP), Tropical Rainfall Measuring Mission (TRMM), global atmospheric reanalysis (ERA-Interim, ERAINT), RegCM4 winds and National Centers for Environmental Prediction (NCEP) reanalysis were used to aid in the understanding of the WAM circulation dynamics. The main WAM circulation features and the general pattern of rainfall in the model simulation compare well with observations. The model simulates the mean rainfall at the peak of the West African summer rainy season (June-July-August), and it captures well the rainbelt associated with the ITCZ. Examination of the intraseasonal variability of rainfall shows that the model captures the three distinct phases of the West African monsoon circulation: onset, intensification and cessation phases. The simulation, for the monthly variability, well depicts the bimodal and unimodal nature of rainfall over southern and northern Ghana respectively. The association between Sea Surface Temperatures (SSTs) and rainfall showed a high positive correlation in most part of the Guinean Coast over the June-July-August (JJA) rainfall season. This depict that a rise in temperatures over the ocean is associated with high rainfall over the coast of West Africa including Ghana.

ACKNOWLEDGEMENTS

The love, support and encouragement from my mum, Mrs. Patience Amoah Jefferson during the study period is highly appreciated.

This research has benefited greatly from the collaboration and co-operation that I enjoyed from my supervisors, Dr. Nana Ama Browne Klutse and Mr. David C. Adukpo. I am very grateful for the opportunity given to me to work with them as a project team member. Above all, they provided me with all the encouragement and support I needed for my studies. I am honour-bound to them than they can imagine.

This thesis was made possible through the United State Agency for International Development (USAID) sponsored Partnership for Enhanced Engagement in Research (PEER) science project which was carried out in the University of Cape Coast. Their platform gave me an opportunity to present my results to local and international conferences and various workshops for criticisms. This helped restructure my thesis. I am most grateful.

I am also indebted to all lectures and staff of the Department of Physics for their support in giving me the knowledge needed for my thesis and also for the peaceful environment they created for me to have a smooth time through my period of study. Words cannot express my sincere gratitude to my friend and colleague, Kwesi A. Quagraine, for the support you gave me to make my study a success. My sincere thanks go to all others who in one way or another contributed to the progress of my studies.

DEDICATION

This work is dedicated to my mum, Mrs. Patience Amoah Jefferson, and my small beloved brother, Godson.

TABLE OF CONTENTS

LIST OF FIGURES

CHAPTER ONE

INTRODUCTION

The West African monsoon is a climatological attribute of major social and economic importance to the population of the region whose economy heavily depends on agriculture. Since rain-fed agriculture is one of the main sources of food and income for the people in West Africa, societies in this region are highly vulnerable to variability in monsoon rains (Baron *et al*. 2005). The sub-Saharan Africa, over the past 40 years, has also been struggling due to a severe drought which has had devastating agricultural, economic and social consequences for the region (Nicholson *et al*. 2000). Due to the warming up of the planet by increasing greenhouse gas concentrations, it is most likely that we can expect changes in the circulation of the African monsoon, which could further influence water resources. Understanding the dynamics and variability at different timescales and most importantly improving our skill in predicting its onset and evolution would contribute toward food security and the stability of the region. For example, information on the timing of the onset of the monsoon, that is, the first rains that are sufficient to provide enough soil moisture at the time of planting would enhance agricultural productivity. Appropriate measures to improve agricultural practices and produce can be put in place if information about the onset of the monsoon is known. The West African summer monsoon (WAM) is known to control the climate of the sub-Saharan West Africa.

The monsoon season, which starts with intense rainfall near the Gulf of Guinea in April, normally remains in place until the end of June. A secondary

precipitation maximum develops near 10^0N in late May. During the last week of June, on average, the coastal precipitation maximum shifts to the latitude of the secondary maximum over a few days. For the rest of the rainy season, the precipitation maximum follows the seasonal cycle fairly accurately. So the monsoon 'jump' can be characterized as the onset of intense convection and rainfall along 10^0N accompanied by its sudden termination along the Guinean coast. This is in sharp contrast with the fact that the ultimate cause of the seasonal migration of the Inter-Tropical Convergence Zone ITCZ, the northward march of the sun, follows a smooth and continuous cycle. The WAM is a complicated system which involves many interactions between the atmosphere, ocean and land surface. The WAM is also influenced by processes that occur over a range of temporal and spatial scales (Hall and Peyrille, 2006). Unfortunately, the global circulation models (GCMs) that are used to make climate projections are currently unable to represent the timing, spatial patterns and magnitude of the monsoon precipitation over West Africa (Yang and Slingo 2001; Dai and Trenberth 2004; Meehl *et al*. 2006). The inability of these models to capture the observed monsoon system greatly undermines their ability to represent potential changes to the monsoon in a warmer climate.

The West African Monsoon (WAM) circulation system (Figure 1) comprises many atmospheric features including the low-level monsoon flow, the African Easterly Jet (AEJ), the African Easterly Waves (AEWs) and the Tropical Easterly Jet (TEJ).

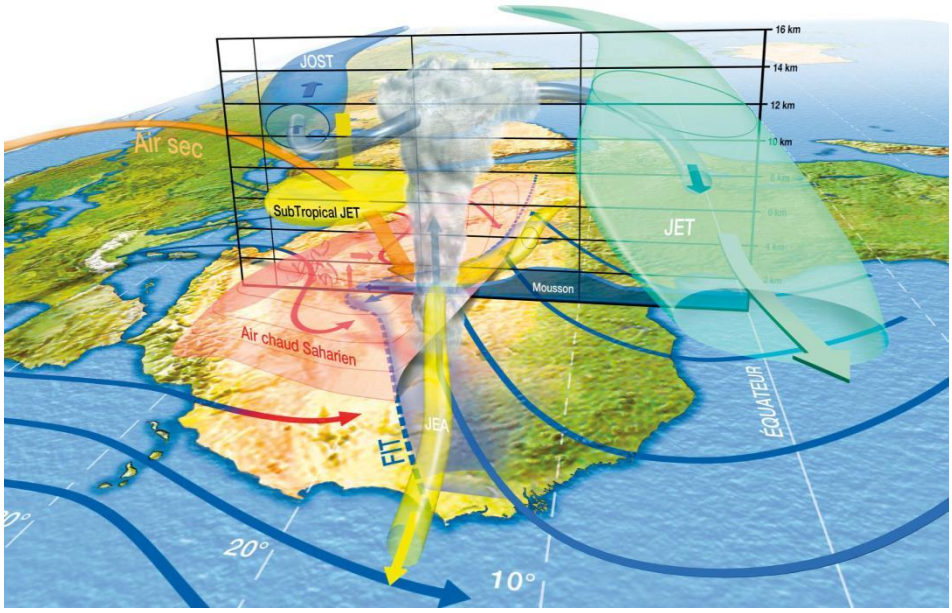

Figure 1: Schematic view of the West African Monsoon System adopted from Lafore *et al.* (2010). FIT stands for ITD (Inter Tropical Discontinuity), "Air chaud Saharien" stands for 'Warm Saharian Air", JEA stands for AEJ (African Easterly Jet), JET stands for TEJ (Tropical Easterly Jet), "Air sec" stands for "Dry Air".

These features interact with each other in a complex way and are responsible for the summer monsoon precipitation over the region. For example, the low-level monsoon flow plays a major role in the transporting of moisture into the West African continent from the Atlantic Ocean; the position and strength of the AEJ, (Figure 1 and 2), cause rainfall variability by transporting moisture away from the continent (Abiodun *et al.*, 2008) and by interacting with mesoscale convective systems embedded in the AEWs (Mohr *et al.*, 2006) while the strength of the TEJ acts mainly in the lifetime of these systems (Jenkins *et al.*, 2005) which are responsible for most of rain over West Africa (Gaye *et al.*, 2005).

Therefore, accurate simulation of its features will help the understanding of its dynamics and variability to improve our skill in predicting its onset and evolution.

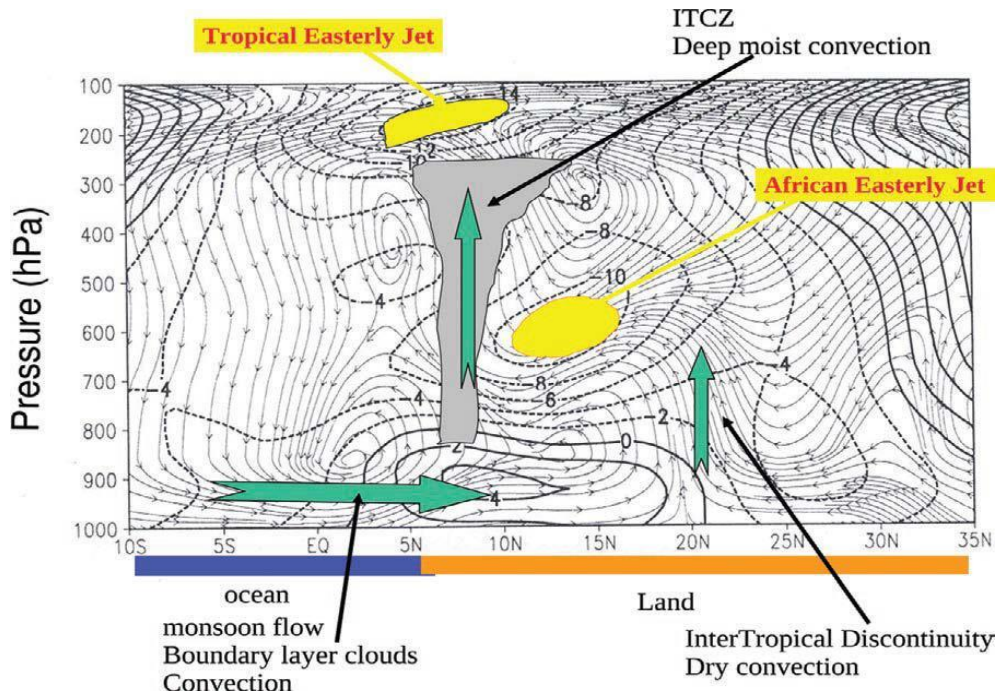

Figure 2: Mean Meridional Circulation (stream lines) and associated mean Zonal Wind (m/s in contours) over West Africa during the summer season adopted from Hourdin *et al*. (2010).

However, since the system comprises atmospheric features that are generated in different locations and sensitive to different topography and surface conditions of the region, selecting the domain size for the regional climate simulation is crucial to get the important sources of forcing features from the boundaries. Regional climate models are driven by time-dependent large-scale meteorological fields specified at the boundaries of the chosen domain. Anthes *et al*. (1989), Giorgi and Mearns (1999) and Browne and Sylla (2012) showed that

the choice of domain size and location affect the balance between the boundary and internal model forcings in the simulation. The location of boundaries in relation to the regional sources of forcings in a particular climatic region can also affect the regional climate model solution (Rauscher *et al*., 2006). As a matter of fact, Seth and Giorgi (1998) showed that the lateral boundaries must be placed well outside the region of interest to avoid unrealistic response to internal forcings while Jones *et al*. (1995) showed that the regional domain must be large enough to allow the full progress of small-scale features over the area of interest. However, Browne and Sylla (2012) showed that the lateral boundaries should be chosen such that the important controls of climate of that region are captured. These indicate that the domain size can have notable effects on the simulation of regional climate models and hence a careful choice of the domain is needed for particular studies.

The West African Climate and its dynamics

West Africa is a region localized between 17^{o}W-10^{o}E and 4^{o}N-20^{o}N. The climate of West Africa is characterized by wet and dry seasons. The length of the dry season over this region is longer than that of the wet season since the rainy season in this region mainly occupies the months of June, July, August and sometimes September. The recent reduction in rainfall is more evident in the last half of the rainy season (August-September). The weather pattern is associated with the northward and southward migration of a narrow zone of reversal in the meridional wind, called the Intertropical Discontinuity (ITD). It is a region of

trade-wind confluence, which produces weak horizontal pressure gradients responsible for weak winds at the surface. Another commonly used term for ITD is the Intertropical Convergence Zone (ITCZ), associated with the zone of maximum convection. Both the ITD and ITCZ exhibit seasonal migration following the seasonal movement of the overhead sun. The wind systems associated with the ITD are characterized mainly by the northeasterly and southwesterly trade winds. During the wet season, the moist southwest monsoon with its maritime characteristics from the Gulf of Guinea invades the region, bringing with it cool breezes. It is often associated with convection and cloudiness. The northeast trade wind, which characterizes the dry period, on the other hand is continental, hot, dry and dust-laden because of its long track from the Sahara desert. During this period, the northeast trade wind blows southwestwards across the region, sometimes reducing visibility to less than 1000 m.

Afiesimama *et al*. (2006) suggested that regional climate models (RCMs) simulate realistic interannual variability of rainfall over West Africa. Patricola and Cook (2010b) assessed that the RCM produces a practical projection of rainfall over much of the northern Africa, with projected summer drought over Guinean Coast. Although RCMs are suitable tools for simulating the WAM, and may offer the best results to understanding climate change over West Africa because of their higher horizontal resolution and ability to resolve small scale atmospheric features (Jenkins *et al*., 2002), they do have limitations.

Challenges in predicting the West African Monsoon System

The better understanding, prediction and simulation of the climate system and its variability at regional and local scales have been a great challenge to the scientific community for many years. The complex nature in climate system is due to the physical processes and activities that occur on space and time scales among the different elements of the climate system. Particularly difficult are the world's monsoon regions where over two thirds of the Earth's populations live. Understanding, simulating and predicting monsoons involves multiple aspects of the physical climate system (i.e., atmosphere, ocean, land, and cryosphere), as well as the impact of human activities in WAM. In this vein, previous studies have used a modelling framework, ranging from conceptual models to fully coupled general circulation models (GCMs) of the ocean-atmosphere-land system to understand the mechanisms involved in monsoon processes and their prediction. The predictability of seasonal and intra-seasonal regional climate over West Africa depends strongly on location, season, and state of global modes of variability that couple to a given region. For example, Ndiaye *et al*. (2011) looked at the behaviour of eight Atmospheric GCMs (AGCMs) and eight coupled atmosphere-ocean GCMs (CGCMs) over the Sahel and determined their levels of correlation between predicted and observed Sahel rainfall at up to 6 month lead time. The same study explored the relative merits of AGCMs versus CGCMs. While there were indications that CGCMs have the advantage over AGCMs, how beneficial this is to skill enhancement remains an open question. Therefore, precise simulation of its features will help the understanding of its dynamics and

variability to enhance our skill in predicting its onset and evolution. Many studies have used regional climate models to understand the WAM system. For instance, Vizy and Cook (2002) studied the response of the WAM to tropical oceanic heating. Jenkins *et al*. (2005) and Sylla *et al*. (2010) investigated the main drivers of the present day and future Sahel droughts. Abiodun *et al*. (2008) documented the impact of deforestation and desertification over West Africa while Moufouma-Okia and Rowell (2010) examined the effect of soil moisture initialization on the WAM simulation. All the studies show a substantial progress in understanding the WAM dynamical and physical features using regional climate models. The potential of the RegCM3 as a tool to study WAM circulation have been highlighted in many studies including (but not limited to) Afiesimama *et al*. (2006), Sylla *et al*. (2009), and Sylla *et al*. (2010). The model has been shown to be capable of reproducing the mean climatology and the variability of the WAM climate.

Nonetheless, the value to society, when translating this measure of predictive skill into the affairs of the decision maker, remains a point of debate. While some positive experiences with using forecasts have led to good lessons (e.g. Tall *et al*. 2012), the interface with decision makers in the view of a variable skill forecast product remains a significant challenge.

The Climate of Ghana

Ghana, a region that shares boundary with the Gulf of Guinea and extends between latitude 4° N and 11° N and longitude 4° W and 2° E, is strongly

influenced by the West African Monsoon. It undergoes various variations in the climate which is marked by severe drought and floods. Ghana's climate is subject to the impact of the Inter-Tropical Convergence Zone and West Africa monsoon. The country is highly vulnerable to climate change, variability and uncertainty. With forests covering around 23 per cent of its territory, Ghana is endowed with abundant natural resources that have played an important role in the agricultural, industrial, economic and social development of the country. Increases in the frequency and intensity of rainfall, floods and landslides, along with the occurrence of extended periods of drought and intense heat, have been linked to changing climatic patterns. Such extreme and unpredictable events have devastating consequences for Ghana's socio-economic development and food security, particularly for the millions of people whose livelihoods depend on agriculture and livestock.

Ghana's rainfall seasons are mostly controlled by the movement of the tropical rain belt, the ITCZ, which swing back and forth between the northern and southern tropics throughout the year. The prevailing wind direction in regions south of the ITCZ is southwesterly, blowing moist air from the Atlantic onto the continent, but on the north of the ITCZ the prevailing winds originate from the northeast, bringing in hot and dusty air from the Sahara desert (known as the 'Harmattan'). As the ITCZ moves from its north and south positions over the year, the zones between these northern and southernmost positions of the ITCZ experience a shift between the two opposing prevailing wind directions. This pattern is known as the West African Monsoon.

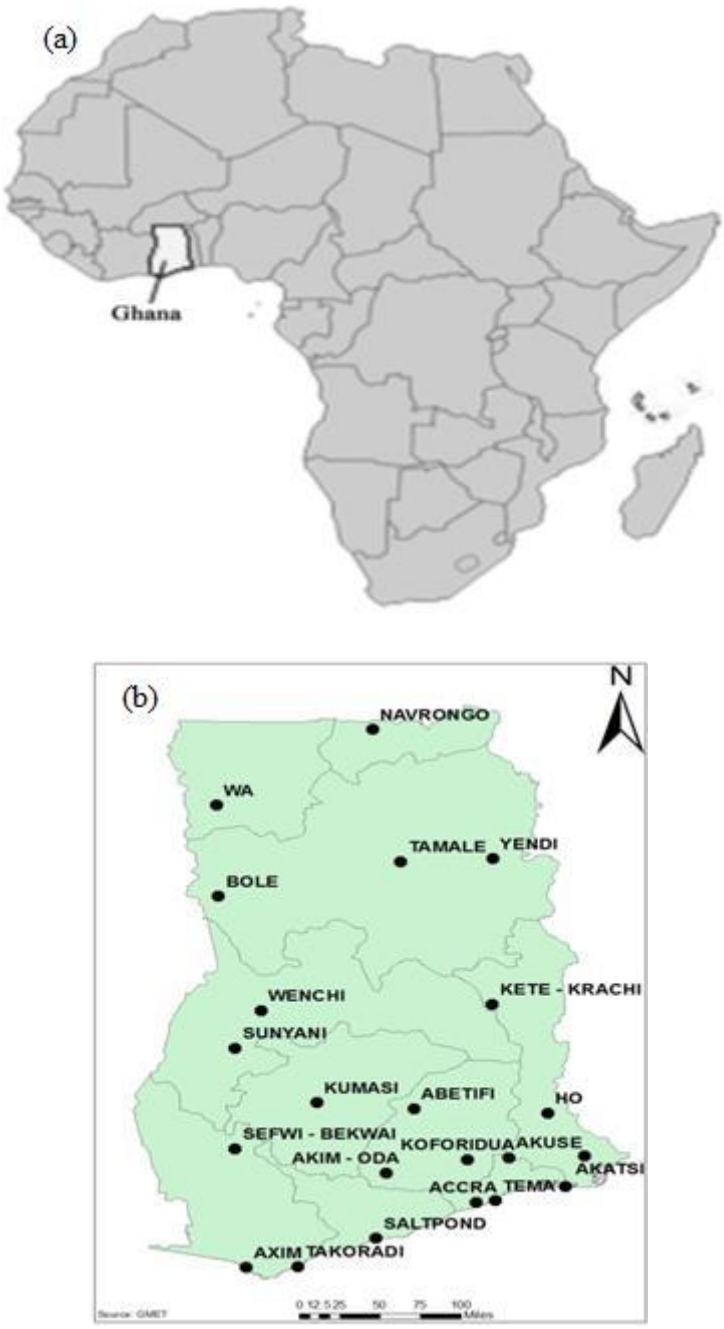

Figure 3: (a) Map of Africa showing Ghana and (b) the map of Ghana showing synoptic weather stations where rain gauge data was obtained (modified from Lacombe, 2012).

The northern part of the region receives 150-250 mm per month in the peak months of the wet season (July to September). The southern parts of Ghana have two wet seasons: the major from March to July, and a minor season in September to November. These seasons correspond to the northern and southern passages of the ITCZ across the region. Studies have shown that the annual rainfall in Ghana is highly variable on inter-annual and inter-decadal timescales (eg. McSweeney *et al*., 2010). This means that there are difficulties in identifying long term trends. The amount of rainfall over Ghana was known to be particularly high in the 1960s. This amount decreased to low levels in the late 1970s and early 1980s, causing an overall decreasing trend in the period 1960 to 2008, of an average 2.3 mm per month (2.4%) per decade (Owusu and Waylen, 2009). The seasonal rainfall in this region varies due to variations in the intensity and movements of the ITCZ, and variations in the intensity and timing of the West African Monsoon. Other factors investigated include variations in the AEJ and the TEJ, (Leroux, 2001; Price *et al*. 2007), and ENSO (Ofori-Sarpong and Annor, 2001). To a certain extent, ENSO is only strongly associated with rainfall in the Sahel with a non-stationary or no clear association with the Guinea Coast region (Ward *et al*. 2004). Seasonal temperature variations in Ghana are greatest in the northern sector, with highest temperatures in the hot, dry season April-May-June (AMJ) at 29-34°C, and lowest in July-August-September (JAS) at 25-29°C. Further south, temperatures reach 25-30°C in the warmest season which is January-February-March (JFM), and 22-25°C at their lowest in JAS.

Approximately 70 per cent of the population depends directly or indirectly on agriculture and forestry, making agriculture and food security particularly vulnerable to climate changes and extremes. Economic assets, in particular cereals that are not tolerant to drought, will be affected by climate trends, compromising the livelihoods of the majority of Ghana's population. Population growth and urbanization mean that periods of drought and flooding place stresses on the availability of water for domestic use. Water deficits have negative impacts on industry, hydro-electric generation and food security. Further risks are related to the higher incidence of malaria and parasitic infections that are linked to flooding.

Majority of research work undertaken on rainfall in Ghana is mostly focused on selected stations or zones (for example, Adiku *et al*. 2007 and Gyau-Boakye and Tumbulto, 2000). In the analysis of the intra-seasonal rainfall variability of Accra and Tamale, Adiku *et al*. (2007) observed the tendency of an intense dry spell during the rainy season in the south (Accra) as compared to that of the north (Tamale). Similar patterns are observed in the analysis of rainfall variability in Tamale (Yengoh, 2010). Friesen (2002) analyzed the spatio-temporal rainfall pattern in northern Ghana, and the result was used to classify the different types of rainfall predominant over the Volta Basin. The rainfall regime characteristics and its variability in the sub-humid region of mid-Ghana is analyzed using daily rainfall data from Wenchi, 1950-2000 (Owusu and Waylen, 2013). Due to the movement of the ITCZ and the influence of the sea surface temperatures (SSTs), the national study of Opoku-Ankomah and Cordery (1994)

suggests that variability in the northern zone is distinct from the other parts of the country.

Research objectives and questions

The main objective of this thesis is to add to our understanding of West Africa Monsoon dynamics. The understanding of the dynamics and variability of the monsoon system at the peak (JJA) of the rainy season will improve our skill in predicting its onset and evolution. Perfection of such prediction would contribute toward food security and the stability of Ghana.

To support the main objective, the thesis addresses the following specific inquiries:

- How well do regional climate models reproduce the circulations that control the climate of West Africa?
- How the West African Monsoon system influences the rainfall over Ghana.
- To what extent does the sea surface temperature contribute to the variability of West African rainfall?

Building on these analyses, the thesis investigates how RegCM4 model reproduce the essential features of the WAM and the relationship those features have with rainfall over Ghana. Information from this research will improve our understanding on how RegCM4 model reproduces the WAM and its influence over Ghana.

Thesis Structure

The thesis is composed of five chapters. After the introductory chapter which gives an overview of the WAM and the climate of Ghana. Chapter 2 covers the climate dynamics of West Africa and climate models. The model and experiments are briefly described in Chapter 3 with the results and analysis discussed in Chapter 4. Chapter 5 is a summary and conclusion of the results and highlights of the contribution of the study to the climatology of Ghana.

CHAPTER TWO

LITERATURE REVIEW

The chapter provides a detailed description of the Climate System as a whole, the dynamics of the West African Climate with highlights on Ghana rainfall variability. A background is provided on the important features that are associated with the climate of West Africa and a discussion on how these features affect the rainfall variability of Ghana is made.

The Climate System

Climate is a statistical description of significant quantities (usually surface variables such as precipitation, temperature and wind) over a period of time ranging from months to thousands or millions of years. Practically, 30 years is used as the standard period defined by World Meteorological Organization to describe the climate. The 30 years was chosen as a period long enough to remove the year-to-year variations in description or application of the climate for one region or the other.

The climate system is an interactive system comprising five major components: the atmosphere, the hydrosphere, the cryosphere, the land surface and the biosphere, which is being forced or influenced by various external forcing mechanisms, with the Sun being the most important mechanism (see Figure 4). Also the direct influence of human activities on the climate system is considered as an external forcing.

The *atmosphere* is the most unstable and rapidly changing part of the system. Its composition, which has changed since the evolution of the Earth, is of central importance to the problem assessed in this work. The Earth's atmosphere is composed mainly of nitrogen (N_2, 78.1% volume mixing ratio), oxygen (O_2, 20.9% volume mixing ratio), and argon (Ar, 0.93% volume mixing ratio). These gases have but limited interaction with the incoming solar radiation and they do not have any interaction with the infrared radiation emitted by the Earth. However, a number of trace gases, such as carbon dioxide (CO_2), methane (CH_4), nitrous oxide (N_2O) and ozone (O_3) do absorb and emit infrared radiation. These so called greenhouse gases, with a total volume mixing ratio in dry air of less than 0.1% by volume, play a very important role in the Earth's energy budget. Moreover, the atmosphere contains water vapour (H_2O), which is also a natural greenhouse gas. Its volume mixing ratio is highly variable, but it is typically in the order of 1%. These greenhouse gases tend to raise the temperature near the Earth's surface due to its absorption of the infrared radiation emitted by the Earth. Water vapour, CO_2 and O_3 also absorb solar short-wave radiation. The atmospheric distribution of ozone and the part it plays in the Earth's energy budget is unique. Ozone acts as a greenhouse gas in the lower part of the atmosphere: the troposphere and lower stratosphere. Higher up in the stratosphere there is a natural layer of high ozone concentration, which absorbs solar ultra-violet radiation. In this way this so-called ozone layer plays an essential role in the balancing of the radiation in the stratosphere and at the same time filter out this potentially damaging form of radiation. Apart from these gases, the

atmosphere also contains solid and liquid particles (aerosols) and clouds, which interact with the incoming and outgoing radiation in a complex and spatially very variable way.

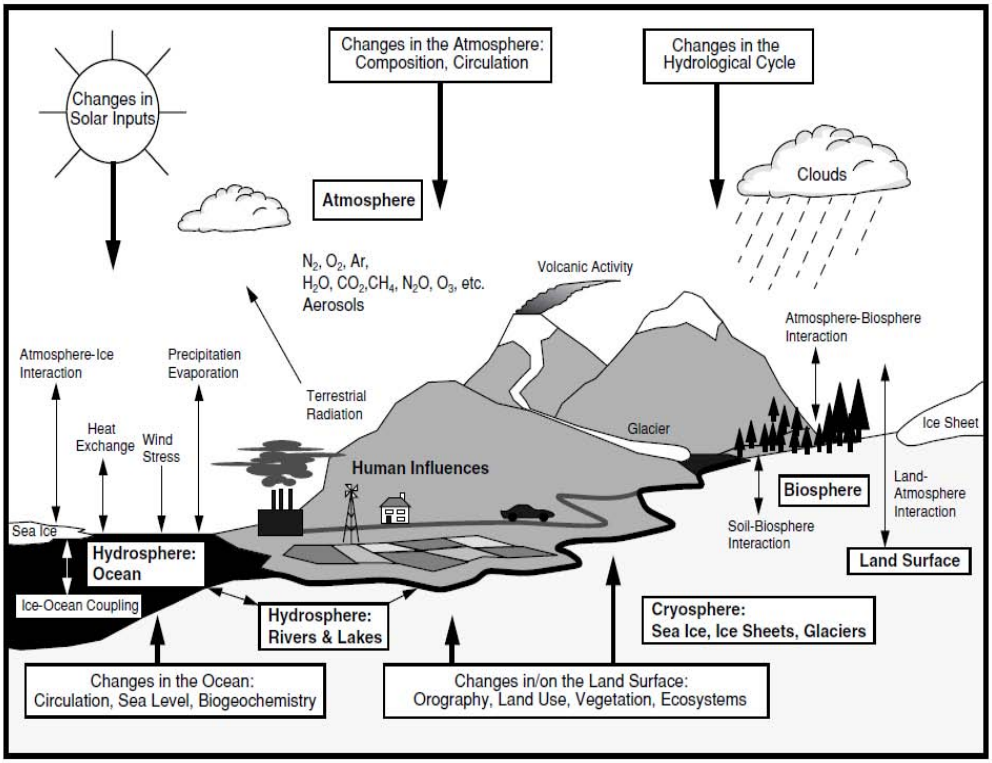

Figure 4: Schematic view of the components of the global climate system (bold), their processes and interactions (thin arrows) and some aspects that may change (bold arrows). (IPCC, 1994: *Climate Change 1994)*

The most variable component of the atmosphere is water in its various phases such as vapour, cloud droplets and ice crystals. Water vapour is the strongest greenhouse gas. For these reasons and because the transition between the various phases absorb and release much energy, water vapour is central to the climate and its variability.

The *hydrosphere* is the component which comprises all liquid surface and subterranean water. Fresh water runoff from the land returning to the oceans in rivers influences the ocean's composition and its circulation. The oceans cover approximately 70% of the Earth's surface. They store and transport a large amount of energy and dissolve and store great quantities of carbon dioxide. Their circulation, which is driven by the wind and density contrasts and caused by salinity and thermal gradients (the so-called thermohaline circulation), is much slower than the atmospheric circulation. Due to the large thermal inertia of the oceans, they damp vast and strong temperature changes and function as a regulator of the Earth's climate and as a source of natural climate variability, in particular on the longer time-scales.

The *cryosphere* derives its importance to the climate system from its high reflectivity (albedo) for solar radiation, its low thermal conductivity, its large thermal inertia and, especially, its critical role in driving deep ocean water circulation. Because the ice sheets store a large amount of water, variations in their volume are a potential source of sea level variations.

Vegetation and soils at the *land surface* control how energy received from the Sun is returned to the atmosphere. Some is returned as long-wave (infrared) radiation, heating the atmosphere as the land surface warms. Some serves to evaporate water, either in the soil or in the leaves of plants, bringing water back into the atmosphere. Soil moisture has a strong influence on the surface temperature. This is because the evaporation of soil moisture requires energy. The roughness of the land surface influences the atmosphere dynamically as winds

blow over the land's surface. Topography and vegetation both determines the roughness. Dust being blown by wind from the surface into the atmosphere interacts well with the atmospheric radiation.

The marine and terrestrial *biospheres* have a major impact on the atmosphere's composition. The biota influences the uptake and release of greenhouse gases. Through the photosynthetic process, both marine and terrestrial plants (especially forests) store significant amounts of carbon from carbon dioxide. Thus, the biosphere plays a central role in the carbon cycle, as well as in the budgets of many other gases, such as methane and nitrous oxide. Other biospheric emissions are the so-called volatile organic compounds (VOC) which may have important effects on atmospheric chemistry, on aerosol formation and therefore on climate. Because the storage of carbon and the exchange of trace gases are influenced by climate, feedbacks between climate change and atmospheric concentrations of trace gases can occur. The influence of climate on the biosphere is preserved as fossils, tree rings, pollen and other records, so that much of what is known of past climates comes from such biotic indicators.

Interactions among the components

Many physical, biological and chemical interaction processes occur among the various components of the climate system on a wide range of space and time scales, making the system extremely complex, although the components of the climate system are very different in their composition. With regard to structure, behaviour, physical and chemical properties, they are all linked by

fluxes of mass, heat and momentum. As an example, the atmosphere and the oceans are strongly coupled and exchange, among others, water vapour and heat through evaporation. This is part of the hydrological cycle and leads to condensation, cloud formation, precipitation and runoff, and supplies energy to weather systems. On the other hand, precipitation has an influence on salinity, its distribution and the thermohaline circulation. Atmosphere and oceans also exchange, among other gases, carbon dioxide, maintaining a balance by dissolving it in cold polar water which sinks into the deep ocean and by outgassing in relatively warm upwelling water near the equator. Some other examples: sea ice hinders the exchanges between atmosphere and oceans; the biosphere influences the carbon dioxide concentration by photosynthesis and respiration, which in turn is influenced by climate change. The biosphere also affects the input of water in the atmosphere through evapotranspiration, and the atmosphere's radiative balance through the amount of sunlight reflected back to the sky (albedo).

Any change, whether natural or anthropogenic, in the components of the climate system and their interactions, or in the external forcing, may result in climate variations. The following sections introduce various aspects of natural climate variations, followed by an introduction to the human influence on the climate system.

Natural Climate Variations

The Sun and the global energy balance

The ultimate source of energy that drives the climate system is radiation from the Sun. About half of the radiation is in the visible short-wave part of the electromagnetic spectrum. The other half is mostly in the near-infrared part, with some in the ultraviolet part of the spectrum. Each square meter of the Earth's spherical surface outside the atmosphere receives an average throughout the year of 342 Watts of solar radiation, 31% of which is immediately reflected back into space by clouds, by the atmosphere, and by the Earth's surface. The remaining 235 Wm^{-2} is partly absorbed by the atmosphere with about 168 Wm^{-2} warming the Earth's surface: the land and the ocean. The Earth's surface returns that heat to the atmosphere, partly as infrared radiation, partly as sensible heat and as water vapour which releases its heat when it condenses higher up in the atmosphere. This exchange of energy between surface and atmosphere maintains under present conditions a global mean temperature near the surface of 14°C, decreasing rapidly with height and reaching a mean temperature of –58°C at the top of the troposphere.

For a stable climate, a balance is required between incoming solar radiation and the outgoing radiation emitted by the climate system. Therefore the climate system itself must radiate on an average of 235 Wm^{-2} back into space. Details of this energy balance can be seen in Figure 5, which shows on the left hand side what happens with the incoming solar radiation, and on the right hand side how the atmosphere emits the outgoing infrared radiation. Of the incoming

solar radiation, 49% (168 Wm^{-2}) is absorbed by the surface. That heat is returned to the atmosphere as sensible heat, as evapotranspiration (latent heat) and as thermal infrared radiation. Most of this radiation is absorbed by the atmosphere, which in turn emits radiation both up and down. The radiation lost to space comes from cloud tops and atmospheric regions much colder than the surface (Kiehl and Trenberth, 1997). This causes a greenhouse effect. Any physical object radiates energy of an amount and at wavelengths typical for the temperature of the object: at higher temperatures more energy is radiated at shorter wavelengths. For the Earth to radiate 235 Wm^{-2}, it should radiate at an effective emission temperature of −19°C with typical wavelengths in the infrared part of the spectrum. This is 33°C lower than the average temperature of 14°C at the Earth's surface. To understand why this is so, one must take into account the radiative properties of the atmosphere in the infrared part of the spectrum.

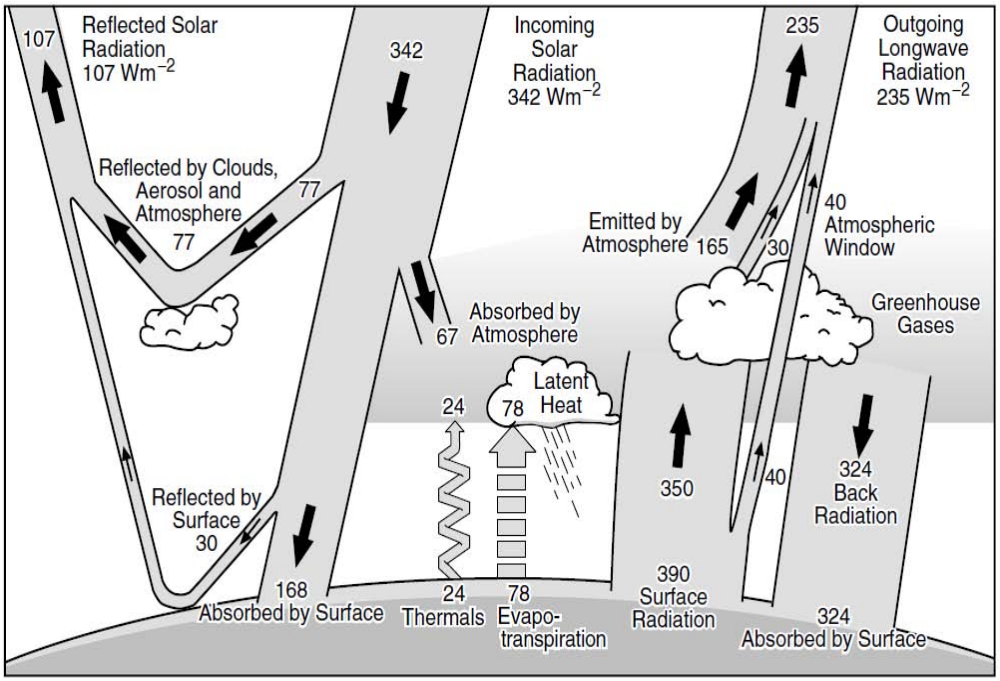

Figure 5: The Earth's annual and global mean energy Budget Source: Kiehl and Trenberth, 1997: Earth's Annual Global Mean Energy Budget, *Bull. Am. Met. Soc*. 78, 197-208.

The natural greenhouse effect

The atmosphere contains several trace gases which absorb and emit infrared radiation. These so-called greenhouse gases absorb infrared radiation, emitted by the Earth's surface, the atmosphere and clouds, except in a transparent part of the spectrum called the "atmospheric window", as shown in Figure 5. They emit in turn infrared radiation in all directions including downward to the Earth's surface. Thus greenhouse gases trap heat within the atmosphere. This mechanism is called the natural greenhouse effect. The net result is an upward transfer of infrared radiation from warmer levels near the Earth's surface to colder levels at higher altitudes. The infrared radiation is effectively radiated back into

space from an altitude with a temperature of, on average, −19°C, in balance with the incoming radiation, whereas the Earth's surface is kept at a much higher temperature with an average value of 14°C. This effective emission temperature of −19°C corresponds in mid-latitudes with a height of approximately 5km. The natural greenhouse effect is part of the energy balance of the Earth, as can be seen schematically in Figure 5.

Clouds also play an important role in the Earth's energy balance and in particular in the natural greenhouse effect. Clouds absorb and emit infrared radiation and thus contribute to warming the Earth's surface, just like the greenhouse gases. On the other hand, most clouds are bright reflectors of solar radiation and tend to cool the climate system. The net average effect of the Earth's cloud cover in the present climate is a slight cooling: the reflection of radiation more than compensates for the greenhouse effect of clouds. However this effect is highly variable, depending on height, type and optical properties of the type of cloud.

Internally and externally induced climate variability

Climate variations, both in the mean state and in other statistics such as, for example, the occurrence of extreme events, may result from radiative forcing, but also from internal interactions between components of the climate system. A distinction can therefore be made between externally and internally induced natural climate variability and change. When variations in the external forcing occur, the response time of the various components of the climate system is very

different. With regard to the atmosphere, the response time of the troposphere is relatively short, from days to weeks, whereas the stratosphere comes into equilibrium on a time-scale of typically a few months.

Due to their large heat capacity, the oceans have a much longer response time, typically decades but up to centuries or millennia. The response time of the strongly coupled surface-troposphere system is therefore slow compared with that of the stratosphere, and is mainly determined by the oceans. The biosphere may respond fast, e.g. to droughts, but also very slowly to imposed changes. Therefore the system may respond to variations in external forcing on a wide range of space- and timescales. The impact of solar variations on the climate provides an example of such externally induced climate variations. But even without changes in external forcing, the climate may vary naturally, because, in a system of components with very different response times and non-linear interactions, the components are never in equilibrium and are constantly varying. An example of such internal climate variation is the El Niño- Southern Oscillation (ENSO), resulting from the interaction between atmosphere and ocean in the tropical Pacific.

The response of the climate to the internal variability of the climate system and to external forcings is further complicated by feedbacks and non-linear responses of the components. A process is called a feedback when the result of the process affects its origin thereby intensifying (positive feedback) or reducing (negative feedback) the original effect. An important example of a positive feedback is the water vapour feedback in which the amount of water vapour in the

atmosphere increases as the Earth warms. This increase in turn may amplify the warming because water vapour is a strong greenhouse gas. A strong and very basic negative feedback is radiative damping: an increase in temperature strongly increases the amount of emitted infrared radiation. This limits and controls the original temperature increase.

A distinction is made between physical feedbacks involving physical climate processes, and biogeochemical feedbacks often involving coupled biological, geological and chemical processes. An example of a physical feedback is the complicated interaction between clouds and the radiative balance. Many processes and interactions in the climate system are non-linear. That means that there is no simple proportional relation between cause and effect. A complex, non-linear system may display what is technically called chaotic behaviour. This means that the behaviour of the system is critically dependent on very small changes of the initial conditions. This does not imply, however, that the behaviour of non-linear chaotic systems is entirely unpredictable, contrary to what is meant by “chaotic” in colloquial language. It has, however, consequences for the nature of its variability and the predictability of its variations. The daily weather is a good example. The evolution of weather systems responsible for the daily weather is governed by such non-linear chaotic dynamics. This does not preclude successful weather prediction, but its predictability is limited to a period of at most two weeks.

Human Influence on the Climate System

Human beings, like other living organisms, have always influenced their environment. It is only since the beginning of the Industrial Revolution, mid-18th century that the impact of human activities has begun to extend to a much larger scale, continental or even global. Human activities, in particular those involving the combustion of fossil fuels for industrial or domestic usage, and biomass burning, produce greenhouse gases and aerosols which affect the composition of the atmosphere. The emission of chlorofluorocarbons (CFCs) and other chlorine and bromine compounds has not only an impact on the radiative forcing, but has also led to the depletion of the stratospheric ozone layer. Land-use change, due to urbanization and human forestry and agricultural practices, affect the physical and biological properties of the Earth's surface. Such effects change the radiative forcing and have a potential impact on regional and global climate. The increase in greenhouse gas and aerosol concentrations in the atmosphere and also land-use change produces a radiative forcing or affects processes and feedbacks in the climate system. The response of the climate to these human-induced forcings is complicated by such feedbacks, by the strong non-linearity of many processes and by the fact that the various coupled components of the climate system have very different response times to perturbations. Qualitatively, an increase of atmospheric greenhouse gas concentrations leads to an average increase of the temperature of the surface-troposphere system. The response of the stratosphere is entirely different. The stratosphere is characterised by a radiative balance between absorption of solar radiation, mainly by ozone, and emission of infrared radiation

mainly by carbon dioxide. An increase in the carbon dioxide concentration therefore leads to an increase of the emission and thus to a cooling of the stratosphere. The only means available to quantify the non-linear climate response is by using numerical models of the climate system based on well-established physical, chemical and biological principles, possibly combined with empirical and statistical methods.

Climate Models

The behaviour of the climate system, its components and their interactions, can be studied and simulated using tools known as climate models. These are designed mainly for studying climate processes and natural climate variability, and for projecting the response of the climate to human-induced forcing. Climate models are mathematical representation of the climate system based on physical, biological and chemical principles (Figure 6). Each component or coupled combination of components of the climate system can be represented by models of varying complexity.

The nucleus of the most complex atmosphere and ocean models, called General Circulation Models (Atmospheric General Circulation Models (AGCMs) and Ocean General Circulation Models (OGCMs)) is based upon physical laws describing the dynamics of atmosphere and ocean, expressed by mathematical equations. Since these equations are non-linear, they need to be solved numerically by means of well-established mathematical techniques. Current atmosphere models are solved spatially on a three-dimensional grid of points on

the globe with a horizontal resolution typically of 250 km and some 10 to 30 levels in the vertical. A typical ocean model has a horizontal resolution of 125 to 250 km and a resolution of 200 to 400 m in the vertical. Their time-dependent behaviour is computed by taking time steps typically of 30 minutes. Models of the various components of the climate system may be coupled to produce increasingly complex models. Processes taking place on spatial and temporal scales smaller than the model's resolution, such as individual clouds or convection in atmosphere models, or heat transport through boundary currents or mesoscale eddies in ocean models are included through a parametric representation in terms of the resolved basic quantities of the model. Coupled atmosphere-ocean models, including such parametrized physical processes, are called Atmosphere-Ocean General Circulation Models (AOGCMs). They are combined with mathematical representations of other components of the climate system, sometimes based on empirical relations, such as the land surface and the cryosphere. The most recent models may include representations of aerosol processes and the carbon cycle, and in the near future perhaps also the atmospheric chemistry. The development of these very complex coupled models goes hand in hand with the availability of ever larger and faster computers to run the models. Climate simulations require the largest, most capable computers available.

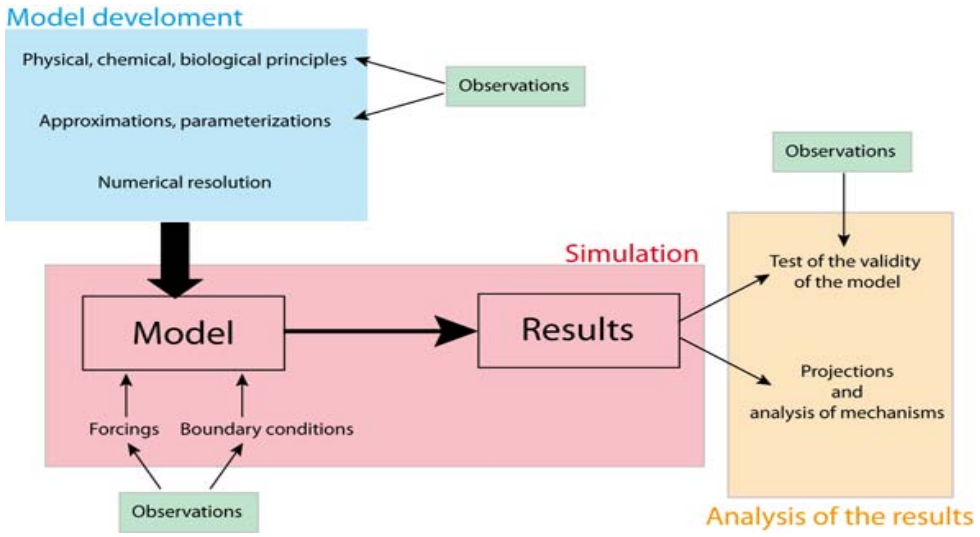

Figure 6: Schematic representation of the development and use of a climate model. Source: Goosse *et al.* (2010)

Even for models with the highest resolution, the numerical grid is still much too coarse to represent small scale processes such as turbulence in the atmospheric and oceanic boundary layers, the interactions of the circulation with small scale topography features, thunderstorms, cloud microphysics processes, etc. Furthermore, many processes are still not sufficiently well-known to include their detailed behaviour in models. As a consequence, parameterizations have to be designed, based on empirical evidence and/or on theoretical arguments, to account for the large-scale influence of those processes not included explicitly. Because these parameterizations reproduce only the first order effects and are usually not valid for all possible conditions, they are often a large source of considerable uncertainty in models.

In addition to the physical, biological and chemical knowledge included in the model equations, climate models require some inputs derived from

observations or other model studies. For a climate model describing nearly all the components of the system, only a relatively small amount of data is required: the solar irradiance, the Earth's radius and period of rotation, the land topography and bathymetry of the ocean, some properties of rocks and soils, etc. On the other hand, for a model that only represents explicitly the physics of the atmosphere, the ocean and the sea ice, information in the form of boundary conditions should be provided for all sub-systems of the climate system not explicitly included in the model: the distribution of vegetation, the topography of the ice sheets, etc.

Those model inputs are often separated into boundary conditions (which are generally fixed during the course of the simulation) and external forcings (such as the changes in solar irradiance) which drives the changes in climate. However, those definitions could sometimes be misleading. Climate models are used to simulate and quantify the climate response to present and future human activities. The first step is to simulate the present climate for extended simulation periods, typically many decades, under present conditions without any change in external climate forcing. The quality of these simulations is assessed by systematically comparing the simulated climate with observations of the present climate. In this way the model is evaluated and its quality established. A range of diagnostic tools has been developed to assist the scientists in carrying out the evaluation. This step is essential to gain confidence in and provide a baseline for projections of human-induced climate change. Models may also be evaluated by running them under different palaeoclimate (e.g. Ice Age) conditions.

Global Climate Models

Global climate models (GCMs) are made up of fundamental laws and parameterisations of physical, chemical and biological components of the climate system. These laws and parameterisations are expressed as mathematical equations, averaged over time and grid volumes. These equations describe the evolution of many variables (e.g. temperature, wind speed, humidity and pressure) and together define the state of the atmosphere. These equations are then changed into a programming language, defining among other things their possible interactions with other formulations, so that they can be solved using computer and integrated forward in discrete time steps.

A global climate model needs to include a number of component models to represent the oceans, atmosphere, land, and continental ice and the fluxes between each other (Figure. 7). Weather models represent a subset of climate models, in which the basic framework of all scales of weather models is presented.

Prior to running any numerical model one requires an initial condition and depending upon the model type one may also require a number of boundary conditions. In numerical weather prediction the initial condition are obtained by analysing and incorporating observations describing the current state of the atmosphere. Whether a grid point is over land or sea, what type of vegetation is prevalent etc, will impact upon how the model interacts with the surface boundary condition.

All numerical models of the atmosphere are based upon the same set of governing equations, describing a number of known physical principles. Where numerical models differ, is how the individual equations are solved; what approximations and assumptions are made and how one represents the physical processes in the physical parameterisations in the atmosphere, for example radiation, convection and precipitation to name a few, often occur at a scale too small to be directly resolved by the numerical model and thus need to be parameterised, i.e., described not by known physical principles, but in an empirical way.

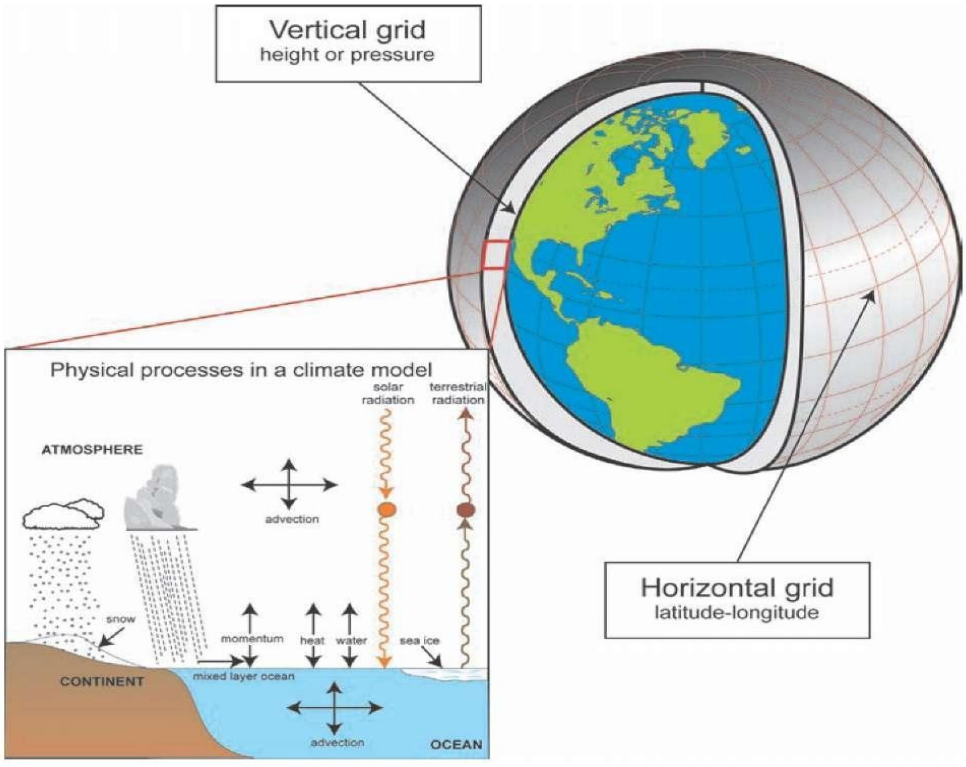

Figure 7: Global Climate Model. Global climate models break the surface down into a series of gridboxes. (World Meteorological Organization: Climate Models)

Using climate models in an experimental manner to improve our understanding of how the climate system works is a highly valuable research application. More often, however, climate models are used to predict the future state of the global climate system. Forecasts (or projections) can be made from a single model forecast, or from an ensemble of forecasts which are produced by slightly perturbing the initial conditions and/or other aspects of the model used. However, one key limitation of Global Climate Models (GCMs) is its fairly coarse horizontal resolution. For the practical planning of water resources, flood defenses etc., countries require information on a much more local scale than what the GCMs can provide. The Regional models provide a solution to this problem.

Regional Climate Models

Simulating climate change at the regional and national levels is essential for policymaking. Only by assessing what the real impact will be on different countries will it be possible to justify difficult social and economic policies to avert a dangerous deterioration in the global climate. Furthermore, understanding processes on the regional scale is a crucial part of global research. Processes acting on local or regional scales such as mountain ranges blocking air flow, or dust clouds interacting with radiation will ultimately have impacts at the global level.

One technique used to overcome the coarse spatial resolution of coupled GCMs is that of nested modeling, depicted in Figure 7. This involves the linking of models of different scales within a global model to provide increasingly detailed analysis of local conditions while using the general analysis of the global

output as a driving force for the higher resolution model. Results for a particular region from a coupled GCM are used as initial and boundary conditions for the RCM, which operates at much higher resolution and often, with more detailed topography and physical parameterizations (Figure. 8). This enables the RCM to be used to enhance the detailed regional model climatology and this downscaling can be extended to even finer detail in local models. This procedure is particularly attractive for mountain regions and coastal zones, as their complexity is unresolved by the coarse structure of a coupled GCM grid.

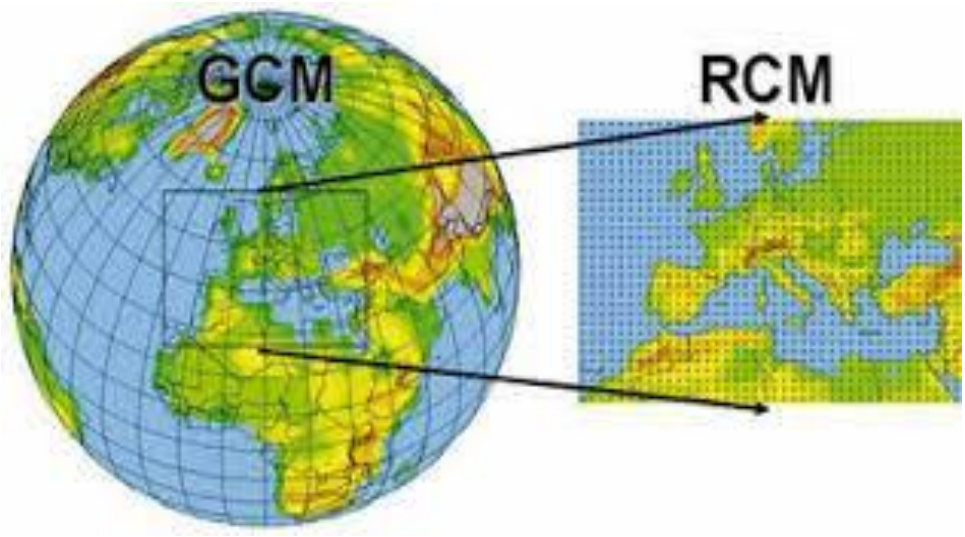

Figure 8: Regional Climate Model Nesting Approach (World Meteorological Organization: Climate Models)

The West African Climate Dynamics

This section looks at the features that cause variations in the West African climate and its effect on rainfall in the region.

The West African Monsoon (WAM) system

The West African Monsoon (WAM) is a major wind system that affects West African regions between latitudes 9° and 20° N and is characterized by winds that blow southwesterly during warmer months and northeasterly during cooler months of the year. The main characteristics of the West African seasons have been known to the scientific community for centuries. The southwest winter monsoon flows as a shallow humid layer of surface air (less than 2,000 metres [about 6,600 feet]) overlain by the primary northeast trade winds, blowing from the Sahara and the Sahel as a deep stream of dry and dusty air. As a surface northeasterly, it is generally referred to as the 'harmattan', cool at night and scorchingly hot by day.

The West African monsoon is the alternation of the southwesterly wind and the harmattan at the surface. This alternation is mostly located between latitudes 9° and 20° N. North easterlies occur constantly farther north, but only south westerlies occur farther south of the equator. Except for erratic rains in the sunny season (June–August), the whole year is mostly dry at 20° N. The drought becomes shorter and less complete farther south. At 12° N it lasts about half the year, and at 8° N it disappears totally. Farther south, a different and lighter drought begins to appear in the sunny months when the monsoonal southwesterly is strongest. This drought results from the arrival of dry surface air issuing from anticyclones formed beyond the equator in the southern hemisphere.

Inter-Tropical Convergence Zone (ITCZ)

The sun's movement from the north to the south of the equator during its annual cycle causes the land and water underneath to warm up. The warm air and water vapor rise to form a slight vacuum; a low-pressure zone. This area formed falls between the trade wind zones along the equator and was originally referred to as the doldrums. Currently, terms that are commonly used include the Inter-tropical Discontinuity (ITD), the Inter-tropical Front (ITF) and the Inter-tropical Convergence Zone (ITZ or ITCZ). This zone is of great importance to agriculture in West Africa, because the rising air and water vapor caused by the heating of the atmosphere by the sun lead to clouds and rainfall. A wave-shaped pattern stretching from east to west across the continent is formed due to the tracking of the sun's movement by the band of rains. The location of the ITCZ is not exactly the same from year to year due to other atmospheric conditions which can speed up or delay the progress of the band of rain. This difference in location of rains can help or destroy crops in their path, particularly the ones in marginal areas, such as the sub-Saharan Sahel zone.

The (ITCZ) is a region of low level convergence, rising air, clouds and rain. Parts of the tropics experience wet seasons when the ITCZ is over or nearby this region. The ITCZ is a global zone with low pressure produced by the convergence of air emanating from the high pressure belt to the north and the high pressure belt to the south of the equator. The parts of the tropics dominated by high pressure have very dry weather and many of the world's deserts are found within this region. The ITCZ shifts position over the course of the year since the

sun's direct rays on the earth vary over the year. The ITCZ tends to be located under and near where the sun's rays are mostly directed. Thus, the ITCZ will be located north of the equator in the Northern Hemisphere summer and south of the equator in the Northern Hemisphere winter. Nonetheless, the mean or average position of the ITCZ is located north of the equator (Figure 9). There is much more landmass in the Northern Hemisphere as compared to the Southern Hemisphere because the ITCZ has a mean position north of the equator.

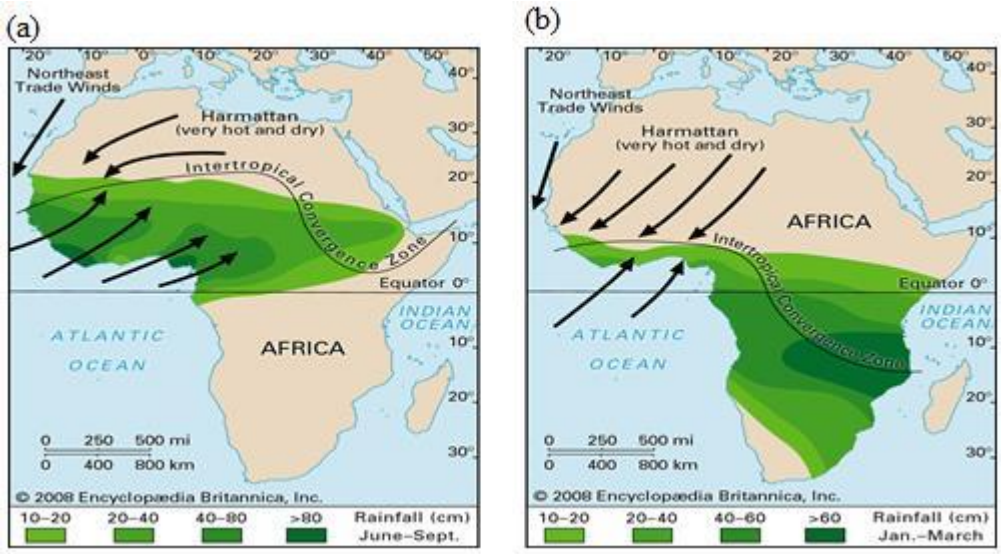

Figure 9: The ITCZ over Africa during (a) June - September and (b) January – March (Encyclopaedia Britannica, 2008)

The African Easterly Waves (AEW)

The African easterly waves (AEWs) are westward-traveling waves that form over northern Africa basically between June and October. It is generally accepted that AEWs arise from instability of the mid-troposphere African easterly jet (AEJ), a prominent feature of the summertime circulation over North Africa. AEWs

modulate West African rainfall, including mesoscale convective systems (MCSs) (Payne and McGarry 1977, Fink and Reiner 2003). These AEWs grow at the expense of the AEJ via a combined barotropic-baroclinic energy conversion process. Burpee (1972) was first to demonstrate that the AEJ satisfies the necessary conditions for baroclinic and barotropic instability (Charney and Stern 1962). They reach their largest amplitude near the west coast of Africa and generally decay after emerging over the eastern Atlantic Ocean 6-8 days after their formation. Substantial variability in AEW structure and evolution occur due to variability on the side of the AEJ on which they form and the intensity and structure of the AEJ. A study by Grist (2001) calculated the quasi-geostrophic potential vorticity (QGPV) gradient based on Charney's (1973) work (Equation 1). The value of the QGPV gradient demonstrated how the easterly wave activity could be influenced by the zonal wind component (i.e. AEJ and TEJ) through barotropic and baroclinic instability. The relevant equation is

$$\frac{\partial \bar{q}}{\partial y} \equiv \underbrace{\beta - \frac{\partial^2 \bar{u}}{\partial y^2}}_{\text{barotropic}} - \underbrace{f_0{}^2 \frac{\partial}{\partial z}\left(\frac{1}{\sigma}\frac{\partial \bar{u}}{\partial z}\right)}_{\text{baroclinic}} \qquad (1)$$

where $\sigma = -\frac{1}{\rho\theta}\left(\frac{\partial \theta}{\partial z}\right)$ and the overbar in equation (2.1) represents the zonal average. Furthermore, equation (1) shows that the QGPV gradient can be broken into two components. The first term corresponds to the vertical shear (barotropic instability) and the second term represents the horizontal shear (baroclinic instability).The relationship between AEWs and rainfall activities arises due to the transportation of convective cells across the region by the AEWs. Laurent *et al*. (1997) noticed that most of the intense rain periods producing about 80% of

the annual rainfall over the region of Niamey, Niger were associated with large cloud clusters which were easily identified as mesoscale convective systems. These convective cells form squall lines which are responsible for the majority of rainfall in the Sahel and West Africa as a whole (Rowell and Milford 1993; Grist 2001). Hamilton and Archbold (1945) first described for West Africa that these squall lines produce heavy rainfall (often >25 mm/hr) and are characterized by a specific and well-defined structure (Mathon *et al*. 2002; Redelsperger and Lafore, 1988; Lafore and Moncrieff, 1989; Zipser, 2003). Squall lines are likely to contribute to a greater share of precipitation in the Sahel, but it is also not easy to find an objective criterion to identify them in a population of MCSs (Mathon *et al*. 2002).

The African Easterly Jet (AEJ)

The AEJ is a mid-tropospheric jet located over much of tropical northern Africa during the northern hemisphere summer. It exhibits large vertical and horizontal wind shears. The vertical wind shear related with the AEJ is crucial to the formation of moist convection and the development of squall lines while both horizontal and vertical wind shears are important for the growth of AEWs. The volume of AEWs increases as a result of the AEJ. The AEJ plays a crucial role in the West African monsoon system and is largely in geostrophic balance.

The AEJ is maintained by two separate meridional circulations (Thorncroft and Blackburn, 1999). The first circulation, associated with dry convection in the Sahara, is characterized by the contrast in sensible heating

between the warm Saharan air over northern Africa and cooler air in the equatorial region. This contrast results in a positive meridional potential temperature gradient that brings forth the strongly vertically-sheared easterly zonal wind between 850-650 hPa associated with the AEJ. The second circulation is associated with deep, moist convection that leads to upper tropospheric heating equator-ward of the AEJ. Burpee (1972) showed that the AEJ is both barotropically and baroclinically unstable resulting in easterly waves which grow at the expense of the jet. This implies that the observed AEJ results from the combination of a diabatically forced meridional circulation that maintains it, and the easterly waves that weaken it (Thorncroft and Blackburn, 1999). The jet develops due to the heating of the West African land mass during the Northern Hemisphere summer which creates a surface temperature and moisture gradient between the Gulf of Guinea, the Sahara and the atmosphere responds by generating vertical wind shear to maintain thermal wind balance. The means by which the African Easterly Jet affect rainfall is by creating divergence of moisture below the level of condensation (Cook, 1999), and hence a decrease in amount of rainfall.

As a first step in understanding the dynamics and generation of the AEJ, we find the degree to which the jet is geostrophic. Here, geostrophy is defined as a balance between the pressure gradient and the local Coriolis accelerations according to

$$\vec{?} = \frac{1}{f} \times \nabla \emptyset. \qquad (2)$$

The ageostrophic wind therefore expresses exactly any local imbalances between pressure gradient and Coriolis forces.

The Tropical Easterly Jet (TEJ)

The tropical easterly jet, or TEJ, is an upper tropospheric easterly jet that extends across the tropics from the eastern Indian Ocean to western Africa. The TEJ is found on the southern boundary of the upper tropospheric anticyclone atop the Tibetan plateau that is associated with the Indian monsoon. The TEJ is weak when the monsoon is weak and strong when the monsoon is strong; suggesting that variability in the monsoon also modulates variability in the strength of the TEJ. The TEJ becomes established once the monsoon has started for the season and decays once the monsoon has ended for the season; thus, it is a salient feature of the tropics only during northern hemisphere summer.

Deep, moist convection forms preferentially in the right entrance and left exit regions of the jet, typically located over Southeast Asia and the northeastern Indian Ocean and central to western Africa, respectively. These regions are those in which upper tropospheric divergence is promoted, as can be demonstrated from concepts of geostrophic and ageostrophic flow. Thus, variability in the intensity, structure and location of the TEJ can impact the development of deep, moist convection. The right entrance region of the j*et al*so happens to correspond to the upward branch of the Walker circulation that extends from Southeast Asia eastward across the Pacific Ocean. Kinetic energy associated with the TEJ forms

preferentially in the upstream region of the jet and is subsequently destroyed in the exit region of the jet.

El Niño-Southern Oscillation (ENSO)

ENSO is a band of anomalously warm ocean water temperatures that occasionally develops off the western coast of South America and can cause climatic changes across the Pacific Ocean. The 'Southern Oscillation' refers to variations in the temperature of the surface of the tropical eastern Pacific Ocean and in air surface pressure in the tropical western Pacific. These two variations are coupled: the warm oceanic phase, *El Niño*, which is accompanied by high air surface pressure in the western Pacific, and the cold phase, *La Niña*, which is accompanied by low air surface pressure in the western Pacific. The oscillations caused by extreme conditions of this climate patterns lead to extreme weather (such as floods and droughts) situations in many regions of the world. Developing countries that depend on agriculture, especially those on the border of the Pacific Ocean, are mostly affected.

Rainfall Variability over West Africa

Many African nations have had to face hard economic and social conditions due to the strong impact caused by the continuous reduction of rainfall in West Africa. Based on collected data, the recent decline in rainfall in West Africa is anomalous to its duration, intensity and seasonal expression (Farmer and Wigley, 1985).

There exist a correlation between interannual rainfall variability in West Africa and patterns of sea surface temperature (SST) anomalies in the tropical Atlantic, Pacific and Indian Oceans (Ward *et al*., 1990; Folland *et al*., 1991; Ward, 1992; Shinoda and Kawamura, 1994; Nicholson and Grist, 2001; Rowell, 2001; Bader and Latif, 2003; Giannini *et al*., 2005). Ward (1992) found that SST forcing from all three major ocean basins may contribute to seasonal Sahelian rainfall variability. The Sahelian rainfall variability is usually associated with warming in the tropical Indian Ocean SST since 1950s (Bader and Latif, 2003).

The El Niño-Southern Oscillation (ENSO) in the tropical Pacific Ocean (e.g., Nicholson, 1997; Nicholson *et al*., 2000; Nicholson and Selato, 2000; Hulme *et al*., 2001) has been agreed upon as one of the more important factors influencing rainfall variability for some regions in Africa and may be more strongly associated with Sahelian rainfall than with that of the Guinea Coast region (Ward *et al*. 2004). Hulme *et al*. (2001) in their detailed analysis of African climate change observed a strong ENSO relationship for equatorial east Africa (high rainfall during a warm ENSO event) and southern Africa (low rainfall during a warm ENSO event), consistent with earlier studies. In Africa, West Africa in particular, there has been a controversy on the influence of the ENSO on rainfall. There is a controversy over its influence in the Sahel although there is a general consensus among researchers on ENSO's influence in some regions, for instance the Guinea coast, where it tends to increase rainfall (Nicholson, 2001). Ward (1992) further noted that ENSO's influence appear to be greater during dry

years than wet years. The different opinion among several authors is due to the complex nature of ENSO's influence in the region.

Significant changes in the intensity and location of the lower and upper tropospheric jets – the African easterly jet (AEJ) and the tropical easterly jet (TEJ) – during the summer monsoon are known to play a very important role in adjusting rainfall over West Africa. Earlier studies (Kanamitsu and Krishnamurti, 1978; Newell and Kidson, 1984) showed a consistent relationship between the AEJ and West Africa rainfall variability. Using a conceptual model for the rainfall variability in the Sahel and comparing its wet (1958-1967) and dry (1968-1997) years, Nicholson and Grist (2001) showed that the location of the AEJ and the associated shear instabilities are the most important local factors controlling Sahel rainfall variability. During wet years, the AEJ is displaced northward by well-developed low-level westerlies. Contrary to this, the dry years are characterized by poorly developed equatorial westerlies, resulting in a southward shift of the AEJ south of the Sahel. The variability of West Africa rainfall is also associated with variations in the well-organized wave disturbance, African easterly waves (AEWs). They are observed to move westward in the lower troposphere of the tropical North Atlantic. Burpee (1972, 1974) found that the westward movement disturbances are concentrated between 5° N and 15° N. The AEW activity occurs during the summer monsoon from June to September with maximum intensity in August. AEWs are generally known to play an important role in modulating daily rainfall over West Africa during the summer monsoon season (Thorncroft, 2001; Fink and Reiner, 2003).

Precipitation patterns

Precipitation patterns for West Africa can generally be divided into two large-scale patterns: a more zonal distribution in the northern part and a distorted southern part (Ojo, 1977). In July the pattern of rainfall distribution is distorted especially south of about latitude 12° N. North of latitude 12°N the usual zonal pattern prevails, but to the south the distribution of rainfall reflects the influence of local conditions. Distortions in the pattern of rainfall distribution are created by such local conditions as the highland and mountainous regions which receive more rainfall than for example the central Ivory Coast and Ghana which receive less than other areas on the same latitude due to orographic effects. The August pattern of rainfall distribution is similar to that of July. However, by September the distorted areas have been greatly reduced and only lie to the south of about latitude 10°N. Thus the pattern is generally more organized than during July and August. In October and November, when the rainy areas are mostly confined to south of approximately latitudes 10°N and 8°N respectively, the pattern becomes more distorted again resembling the structure at the beginning of the rainy season. October and November represent the beginning of the dry season and the decrease in rainfall at this time is mainly because the ITCZ has moved so far south that only parts of the Guinean Coast.

Traditionally, rainfall is classified into three main categories of Convectional, Cyclonic/Frontal, and Relief/Orographic rainfall, according to the mechanism involved in the vertical displacement of air and subsequent adiabatic cooling and condensation. In the tropics, with particular reference to West Africa,

this system of classification is inadequate in terms of current knowledge of the region's precipitation dynamics.

To start with, there is no evidence of cyclonic or frontal activity in West Africa. To add to that, large amounts of rainfall are produced by atmospheric processes other than convection and orographic uplift. In some areas, over 50 per cent of the total annual rainfall is derived from these extra sources. Within the test area, there are three rainfall origins to be found. Convective systems divided into local rainstorms and line squalls as well as convergence rainfall due to monsoonal air layers.

Monsoon rains

Between July and September, most areas of West Africa south of 10°N experience widespread and prolonged "monsoon" rains. Periods of maximum convergence rainfall coincide with minimal thunderstorm activity which tends to suggest differences in the mechanisms that organize the thunderstorm and the massive uplift of monsoon air. Characteristic for this convergence rainfall is that, apart from affecting wide areas at a time, it occurs in light, continuous downpours with occasional spells lasting from a few hours to several days.

CHAPTER THREE

MODELS, DATA, AND METHODS

This chapter provides a description of the models, data and methods used in the study. It begins with a concise description of the model used followed by a brief description of the observation data from the Ghana Meteorological Agency in the study. A summary of the simulations is then provided.

Regional Climate model - Version 4 (RegCM4)

The regional climate model used in this study is the RegCM4 which is the enhanced version of the RegCM3 (Pal *et al*. 2007) and the RegCM2 (Giorgi *et al*., 1993a, b). It is a hydrostatic limited area model, with finite-difference discretization and a sigma coordinate in the vertical. The RegCM was the first limited area model developed for long-term regional climate simulation: it has been used in numerous regional model intercomparison projects, and it has been applied by a large community for a wide range of regional climate studies, from process studies (Qian 2008, Qian *et al*. 2010) to paleo-climate and future climate projections (Giorgi and Mearns, 1999, Giorgi *et al*. 2006).

Model Description

Dynamics

The model dynamic equations and numerical discretization are described by Grell *et al.* (1994).

Horizontal Momentum Equations:

$$\frac{\partial u}{\partial t} = -u^2 \left(\frac{\partial u / m}{\partial x} + \frac{\partial u / m}{\partial y}\right) - \frac{\partial u}{\partial \sigma}$$

$$- RT_v \left[\frac{\partial p^*}{\partial x} + \frac{\partial \phi}{\partial x}\right] + fv + F_H u + F_v$$

$$(p^* + p_t)\sigma \quad \partial x \quad \partial x \qquad (3)$$

$$\frac{\partial v}{\partial t} = -u^2 \left(\frac{\partial v / m}{\partial x} + \frac{\partial v / m}{\partial y}\right) - \frac{\partial v}{\partial \sigma}$$

$$- RT_v \left[\frac{\partial p^*}{\partial y} + \frac{\partial \phi}{\partial y}\right] + fu + F_H v + F_v$$

$$(p^* + p_t)\sigma \quad \partial y \quad \partial y \qquad (4)$$

where *u* and *v* are the eastward and northward components of velocity, *Tv* is virtual temperature, ∅ is geopotential height, *f* is the coriolis parameter, *R* is the gas constant for dry air, *m* is the map scale factor for either the Polar Stereographic, Lambert Conformal, or Mercator map projections, $\sigma = \frac{\partial \sigma}{\partial t}$ and F_H and F_v represent the effects of horizontal and vertical diffusion respectively, and $p^* = p_s - p_t$.

Continuity and Sigma dot (σ̇) Equations

$$\frac{\partial p^*}{\partial t} = -u^2 \left(\frac{\partial p^* / m}{\partial x} + \frac{\partial p^* / m}{\partial y}\right) - \frac{\partial p^* \dot{\sigma}}{\partial \sigma} \qquad (5)$$

The vertical integral of Equation 5 is used to compute the temporal variation of the surface pressure in the model,

$$\frac{\partial p_s}{\partial t} = -g \int_0^1 \left(\frac{\partial p}{\partial x} u_m + \frac{\partial p}{\partial y} v_m \right) d\sigma \qquad (6)$$

After calculation of the surface-pressure tendency $\frac{\partial p_s}{\partial t}$, the vertical velocity ($\dot{\sigma}$) in σ coordinates is computed at each level in the model from the vertical integral of Equation 5.

$$\dot{\sigma} = -\frac{1}{p} \int_0^{\sigma} \left[\frac{\partial p_s}{\partial t} + g \left(\frac{\partial p}{\partial x} u_m + \frac{\partial p}{\partial y} v_m \right) \right] d\sigma' \qquad (7)$$

where σ' is a dummy variable of integration and $\dot{\sigma}_{\sigma=0} = 0$.

Thermodynamic Equation and Equation for Omega (ω)

The thermodynamic equation is

$$\frac{\partial T}{\partial t} = -g \left(\frac{\partial T}{\partial x} u_m + \frac{\partial T}{\partial y} v_m \right) - \frac{\partial T}{\partial p} \dot{\sigma} + \frac{RT}{c_p (\sigma + p'/p)} + \frac{Q}{c_p} + F_H + F_V \qquad (8)$$

where c_p is the specific heat for moist air at constant pressure, Q is the diabatic heating and θ is

$$\theta = T + \sigma \frac{\partial T}{\partial p} \qquad (9)$$

where,

$$\frac{\partial \sigma}{\partial t} = \frac{\partial \sigma}{\partial t} + m\left(u\frac{\partial \sigma}{\partial x} + v\frac{\partial \sigma}{\partial y}\right) \quad (10)$$

The expression for $c_{pm} = c_p(1+0.8q_v)$, where c_p is the specific heat at constant pressure for dry air and q_v is the mixing ratio of water vapor.

Hydrostatic Equation

The hydrostatic equation is used to compute the geopotential heights from the virtual temperature *Tv*,

$$\frac{\partial \phi}{\partial \ln(\sigma + p/p^*)} = -RT_v\left(1 + \frac{q_v + q_r}{1 + q_c}\right)^{-1} \quad (11)$$

where $T_v = T(1 + 0.608q_v)$, q_v, q_c, and q_r are the water vapor, cloud water or ice, and rain water or snow, mixing ratios.

Radiation Scheme

Calculations of the radiative transfer in Regional Climate Model 4 (RegCM4) are accomplished with the radiative transfer scheme of the global NCAR Community Climate Model 3 (CCM3) (Kiehl *et al*. 1996), as resolved by Giorgi *et al*. (1999). This includes computing for the short-wave and infrared parts of the spectrum, as well as both atmospheric gases and aerosols. The scheme entails contributions from all main greenhouse gases, i.e. H_2O, CO_2, O_3, CH_4, N_2O, and CFCs, and solar radiative processes are conducted using a delta-Eddington formulation (Briegleb 1992). Absorption and scattering of solar radiation by aerosols are also involved based on the aerosol optical properties (absorption coefficient and single scattering albedo).

For cloud radiation, the solar spectrum optical properties rely on the cloud liquid water path, which in turn rely upon the cloud liquid water amount which is anticipated to be calculated by the model, cloud fractional cover, which is computed characteristically as a function of relative humidity, and effective cloud droplet radius, which is parameterized to be a function of temperature and land sea mask for liquid water and as a function of height for ice phase. In addition, the scheme characteristically computes a fraction of cloud ice as a function of temperature. In the infrared spectrum, the cloud emissivity is computed as a function of cloud liquid/ice water path and cloud infrared absorption cross sections based on effective radii for the liquid and ice phases. One problem with this formulation is that the scheme uses the cloud fractional cover to produce grid box mean cloud properties which are then treated as though the entire grid box were covered by an effectively thinner cloud layer.

However, the non-linear nature of radiative transfer tends to produce a 'grayer' mean grid box than if separate cloudy and clear sky fractional fluxes were calculated. By taking advantage of the fact that the scheme also computes clear sky fluxes for diagnostic purposes, in RegCM4 we adjusted this radiative cloud representation by calculating first the total cloud cover at a given grid point and then calculating the surface fluxes separately for the cloudy and clear sky portions of the grid box. The total cloud cover at a model grid box is given by an intermediate value between the one obtained using the random overlap assumption (which maximizes cloud cover) and that given by the largest cloud cover located in any single layer of the column overlying the grid box (which

implies a full overlap and thus it is a minimum estimate of total cloud cover). This improvement thus accounts for the occurrence of fractional clear sky at a given grid box, leading to more realistic grid-box average surface radiative fluxes in fractional cloudy conditions.

The other main development that can be compared to RegCM3 is the aerosol radiative transfer calculations. In RegCM3, the aerosol radiative forcing was based on 3-dimensional fields produced by the aerosol model, and included only scattering and absorption in the shortwave spectrum (Giorgi *et al*. 2002). In RegCM4, there was an additional contribution of the infrared spectrum following Solmon *et al*. (2008). This is very necessary for relatively large dust and sea salt particles. It is calculated by introducing an aerosol infrared emissivity calculated as a function of the aerosol path and absorption cross section estimated from aerosol size distribution and long-wave refractive indices. Long-wave diffusion, which could be relevant for larger dust particles, is not treated as part of this scheme.

Land Surface Model

Since the first version of the RegCM, land surface processes have been described via the Biosphere-Atmosphere Transfer Scheme (BATS) of Dickinson *et al*. (1993). This scheme, which has been used for many years, includes a 1-layer vegetation module, a 1-layer snow module, a force-restore model for soil temperatures, a 3-layer soil scheme, and a simple surface runoff parameterization. The scheme comprises 20 surface types and 12 soil color and soil texture types.

Furthermore, a sub-grid land surface configuration can be used by which each model grid point is divided into a regular sub-grid, and land surface processes are calculated at each sub-grid point taking into account the local land-use and topography (Giorgi *et al*. 2003). This latter scheme was shown to be especially useful in improving the simulation of the surface hydrologic cycle in mountainous areas (Giorgi *et al*. 2003).

As a first augmentation, in RegCM4, 2 new land use types were added to BATS to represent urban and suburban environments. Urban development not only modifies the surface albedo and alters the surface energy balance, but also creates impervious surfaces with large effects on runoff and evapotranspiration. These effects can be described by modifying relevant properties of the land surface types in the BATS package, such as maximum vegetation cover, roughness length, albedo, and soil characteristics. For this purpose, we implemented the parameters proposed in Table 1 of Kueppers *et al*. (2008).

The second major addition to RegCM4 is the option to use the Community Land Model (CLM), version 3.5 (Tawfik and Steiner 2011). Compared to BATS, CLM is a more advanced package, which is described in detail by Oleson *et al*. (2004, 2008). It uses a series of biogeophysically-based parameterizations to describe the land–atmosphere exchanges of energy, momentum, water, and carbon. Within each RegCM4 grid cell, CLM3 divides the cell area into a first sub-grid hierarchy composed of land units (glacier, wetland, lake, urban, and vegetated land cover), and a second and third sub-grid hierarchy for vegetated land units, including different snow/soil columns for the different vegetation

fractions, and plant functional types (PFTs; Oleson *et al*. 2004). Biogeophysical processes are calculated for each land unit, column, and PFT separately, and then averaged for return to the atmospheric model. CLM3 biogeophysical calculations include a coupled photosynthesis–stomatal conductance model, in-canopy radiation schemes, revised multi-layer snow parameterizations, and surface hydrology including a distributed river runoff scheme (Oleson *et al*. 2008). Soil temperature and water content are calculated with the use of a multiple layer model. Being much more complex than BATS, the use of CLM adds about 20% to the computing time necessary to run the model, depending on the fraction of land points in the domain. CLM also has an option for describing interactive vegetation; however, this has not been tested yet within the RegCM4 framework. CLM was shown to substantially affect the land–atmosphere exchanges of moisture and energy and the associated surface climate feedbacks compared to BATS (Steiner *et al*. 2009).

Convective schemes

The convective precipitation parameterizations used in this study are the modified-Kuo (Anthes, 1977) and the Grell (1993) schemes. In the Grell (1993) scheme deep convective clouds are represented by an updraft and a downdraft that are undiluted and mix with environmental air only in the base and top of the cloud. The heating and moistening profiles are derived from the latent heat release or absorption, linked with the updraft–downdraft fluxes and compensating motion. The Grell scheme convective closure assumption can be of two types.

Two different closures can be adopted: an Arakawa-Schubert type closure in which all buoyant energy is immediately released at each time step and a Fritsch-Chappell type closure in which the available buoyant energy is released with a time scale typically on the order of 30 min. The Kuo scheme assumes that convection is started under conditions of convective instability and moisture convergence in the vertical column. Part of this moisture convergence precipitates and the rest is used to moisten the atmosphere. In the vertical a parabolic profile is used to distribute the latent heat of condensation, so that the maximum heating is located in the upper half of the cloud (Anthes, 1977).

A major augmentation in RegCM4 compared to previous versions of the model is the capability of running different convection schemes over land and ocean, a configuration which we refer to as 'mixed convection.' Extensive test experiments showed that different schemes have different performance over different regions and in particular over land versus ocean areas. For example, the Massachusetts Institute of Technology (MIT) scheme tends to produce excessive precipitation over land areas, especially through the occurrence of very intense individual precipitation events. In other words, once the scheme is activated, it becomes difficult to 'decelerate.' Conversely, it was found that the Grell scheme tends to produce excessively weak precipitation over tropical oceans. These preliminary tests suggested that a mixed convection approach by which, for example, the MIT scheme is used over oceans and the Grell scheme over land might be the most suitable option to pursue, and therefore this option was added to the model. It was also note that, as in the previous version (RegCM3) and many

other schemes, these cumulus parameterizations tend to maximize rain in the early afternoon, essentially in response to the surface heating by the solar cycle. This often leads to an earlier than observed diurnal precipitation maximum over tropical regions (Diro *et al*. 2012).

Resolved scale precipitation

The resolved scale precipitation scheme is essentially based on the subgrid explicit moisture scheme (SUBEX) parameterization of Pal *et al*. (2000) and includes a prognostic equation for cloud water. It first calculates fractional cloud cover at a given grid point based on the local relative humidity. Then, in the cloudy fraction it uses a Kessler-type bulk formulation in which cloud water is turned into precipitation via an autoconversion and an accretion term. Below-cloud evaporation of falling raindrops is also accounted for based on the local relative humidity and an evaporation rate coefficient. Key sensitivity parameters in this scheme are the in-cloud liquid water threshold for the activation of the autoconversion term (Qth) and the rate of sub-cloud evaporation (Cevap). Greater values of Qth and Cevap lead to decreased precipitation amounts. Traditionally, RegCM3 has shown a tendency to produce excessive precipitation, especially at high resolutions (Im *et al*. 2010, Torma *et al*. 2011), and optimizations of these parameters have proven effective in ameliorating this problem (see Torma *et al*. 2011).

The observation and reanalysis data

The following available observation and reanalysis dataset were used to validate the RegCM4 model.

Meteorology Station Data

Data for monthly total rainfall for twenty two synoptic stations (Figure 3b) were collected from Ghana Meteorological (GMet) Agency for a 13-year period, which is from 1998 to 2010. Average of these data was calculated to arrive at the mean rainfall amounts over the northern, middle and southern belts of Ghana.

National Centers for Environmental Prediction reanalysis 1 Data

The National Centers for Environmental Prediction/National Center for Atmospheric Research (NCEP/NCAR) reanalysis dataset (Kalnay *et al*. 1996) of the Climate Diagnostics Center (CDC) of the National Oceanic and Atmospheric Administration (NOAA) uses a state-of-the-art analysis/forecast system to perform data assimilation using past data from 1948 to the present. The dataset is available as 4 time daily format and as daily averages. The data is available also in monthly means with a resolution of 2.0^{o} x 2.0^{o} latitude-longitude grid and has 17 pressure and 28 sigma levels. The NCEP data was used to validate the model for the circulation systems. These are used in the seasonal and inter-annual analyses in terms of monthly mean from 1971 to 2000. The meteorological fields utilized at seasonal time scale are precipitable water, zonal (U) and meridional

(V) components of the wind (ms^{-1}), mean sea level pressure (hPa), geopotential height (m) and air temperature (K).

NCEP reanalysis data have been used by many researchers and their qualities have been documented (WMO/D-NO.876, 1997). For example, Cavalcanti *et al.* (1998) studied years of contrasting characteristics using NCEP reanalysis data. Their analysis was based on anomaly fields of precipitation, zonal and meridional components of the wind at 200 hPa, outgoing longwave radiation (OLR) and specific humidity. Moisture divergence and transport were calculated in the layer 1000 hPa to 300hPa. They analyzed four periods of summer and autumn seasons of the dry years 1983 and 1993 in the Northeast Region of Brazil and wet years 1984 and 1994. They observed that results of circulation patterns during these opposite cases were consistent in terms of precipitation observed over Brazil. The differences in atmospheric variables between dry and wet periods defined clearly the characteristics of the atmosphere. Mo *et al.* (1998) also used NCEP reanalysis data and forecasts to examine the atmospheric circulations associated with California rainfall anomalies. They used global gridded analysis of outgoing longwave radiation (OLR) from NCEP covering the period 1973-1995. Their results showed that the six hour precipitation forecasts are able to capture signals associated with inter-annual variability.

In the report from the first World Climate Research Programme (WCRP) international conference on reanalysis that was held at NOAA, USA, NCEP reanalysis data are of high quality and undertaken with fixed state-of-the-art data assimilation/analysis methods to provide multi-year global datasets for a range of

investigations of many aspects of climate, particularly inter-annual variability and for model validation and predictability studies. The large spurious effects present in operational analyses arising from changes in assimilation systems are absent from these datasets which thus provide a more homogeneous time series for precipitation, diabatic heating, surface fluxes and other components of the hydrological cycle (WWO/TD-NO. 876, 1997).

However, one problem with the NCEP reanalysis is the assimilation of surface data over Africa. Evidently, to reduce artificial boundary layers in the model observed fields, only station pressure data are incorporated. Wind, temperature, rainfall and other valuable inputs are ignored. Upper air radiosonde, aircraft and satellite data are incorporated; but the radiosonde network is very sparse over Africa. Hence further model improvements could bring a greater degree of realism to the reanalysis fields.

ERA-Interim (ERAINT)

ERA-Interim is the latest global atmospheric reanalysis, which was produced by the "European Centre for Medium Range Weather Forecasts" (ECMWF). The ERA-Interim-project was carried out to replace the previous atmospheric reanalysis ERA-40. So far it dates back to 1979 and has been continued to the present. Problems that occurred in ERA-40 have been treated with improved methods in this new reanalysis. The identified problems were the hydrological cycle, the quality of the stratospheric circulation, and the time consistency of the analyzed fields. The number of pressure levels from ERA-40

has been increased from 23 to 37 levels and additional cloud parameters are included.

The Global Precipitation Climatology Project (GPCP)

The Global Precipitation Climatology Project (GPCP) is maintained by the National Aeronautics and Space Administration (NASA) and provides daily rainfall for each 1° on the globe from October 1996 to August 2009. In order to derive rainfall estimates, GPCP incorporates a blend of the six best quasi-global datasets (Huffman *et al*. 2001). In particular, these datasets are: 1) Special Sensor Microwave/Imager (SSM/I; fractional occurrence of precipitation), 2) GPCP Version 2.1 Satellite-Gauge (monthly accumulation of precipitation), 3) geosynchronous orbit IR brightness temperature histograms, 4) low-orbit IR GOES Precipitation Index (GPI), 5) Television and Infrared Operation Satellite (TIROS) Operational Vertical Sounder (TOVS), and 6) Atmospheric Infrared Sounder (AIRS). The use of high resolution precipitation data over West Africa is important to account for topographical variances and the sharp moisture gradient between the Gulf of Guinea and the Sahara.

Experiment Design

The regional model (RegCM4) is integrated over the West African domain for the 13-year period from January 1998 through December 2010 at a spatial resolution of 25 km with 18 vertical levels. The domain exhibits some localized highlands around Cameroun (Cameroun Mountain), Central Nigeria (Jos Plateau)

and Guinea (Guinea Highlands). In validating rainfall and wind for the model in Chapter 4 of the study, GPCP, TRMM, ERAINT and NCEP were used for comparisons: the simulated winds are validated with NCEP reanalysis (2.0^{o} x 2.0^{o} resolution; Kalnay *et al*, (1996) whiles the simulated precipitation is validated against two observational datasets: GPCP (2.5° × 2.5° resolution; Adler *et al*. (2003), TRMM (Tropical Rainfall Measuring Mission, 0.25° × 0.25° resolution; Mitchell *et al*. (2004). TRMM is satellite-derived daily and monthly rainfall providing data for the entire tropics since November 1997. Although both observational data are mainly based on satellite observations, they have also been compared and merged with ground station rain gauges to create the final products. These simulation and observations are then analyzed using Ferret, an interactive computer visualization and analysis environment, to view and analyze the results. Average monthly rainfall amount over Ghana from 1998 to 2010 is analyzed using the GMet data. In particular, the analysis focuses on the intraseasonal and interannual variability of rainfall and the influence of related circulation features such as wind over West Africa have had on Ghana.

Study Domain

This thesis focuses on West Africa, 20°W to 20°E and 0°N to 25°N, and its monsoon circulation features. A more localized region, Ghana, is then analyzed to know the impact the West African Monsoon circulation have on Ghana.

CHAPTER FOUR

RESULTS AND DISCUSSION

In this chapter, we examine and compare the mean rainfall variability over West Africa from GPCP and TRMM observations, ERAINT reanalysis with the REGCM4 simulation. The simulated synoptic circulation features, such as AEJ and TEJ, are compared with NCEP dataset. We show results for June, July and August (JJA) for a 13-year period, 1998 – 2010. Our focus on JJA is due to the fact that it is the peak of the monsoon season and an essential period for the West African economy and thus a critical period for a good simulation. The ocean effect on West African rainfall through South Atlantic SST is studied and reported.

Atmospheric Dynamics associated with the West African rainfall

In this section, a comparison of the zonal wind simulated by the NCEP reanalysis and the RegCM4 from 1998 to 2010 was carried out. Four seasons are considered: December to February (DJF), March to May (MAM), June to August (JJA) and September to November (SON). Figure 10 shows the vertical cross section of the zonal wind averaged between 20°E and 20°W and for the whole period of simulation (1998–2010). In DJF, the core of the AEJ (~ $8ms^{-1}$) is located around 4°N at 600 hPa in both the reanalysis and the model. At lower levels from 1000 hPa to 800 hPa, a well-known southward flow (*i.e*. the Harmattan) is simulated between 12°N - 20°N. The model showed a good representation of the position of the westerlies. In MAM, the core of the AEJ (~ $10ms^{-1}$) increased and

moved northward up to 8°N in the reanalysis. The model maintained its AEJ core (~ 8ms^{-1}) but moved northward up to 8°N. It was noted by Grist and Nicholson (2001) that this latitudinal shift may explain the seasonal fluctuation of the maximum of the wind shear. Additionally, positive values of the zonal wind in the lower levels are related to a latitudinal extent of the monsoon flow from the Atlantic Ocean to the Sudanese zone with higher values over the Guinean region.

In JJA, NCEP shows the monsoon flow winds below 800 hPa at 2–19 °N at lower levels. The AEJ at 600hPa with a core of 10ms^{-1} moved northward as compared to the previous season. The AEJ which is located around 14°N at the tropospheric mid-levels (600 hPa) appears as a result of the strong meridional surface moisture and temperature gradients between the Sahara and equatorial Africa (Cook, 1999; Thorncroft and Blackburn, 1999). In the upper tropospheric levels at 200 hPa, the TEJ is centered at 6°N and is associated with the upper-level outflow from the Asian monsoon. An intensification of the TEJ is observed at 200 hPa as compared to the TEJ in DJF and MAM. The regional climate model captures reasonably well the low level winds below 800 hPa but the monsoon flow is somewhat overestimated. The monsoon flow is a major source of water vapor for West Africa and the importance for a model to capture it well cannot be overestimated. The AEJ is clearly simulated at 600 hPa and around 15°N but its strength is weaker by about 2ms^{-1} with respect to the NCEP. On the other hand, the regional model shows a stronger TEJ in the upper level. As discussed in Gallee *et al*. (2004) and Sylla *et al*. (2009), the variation in the strength of the

westerlies and jets between the regional model and the reanalysis data may be due to differences in the simulated temperature gradients.

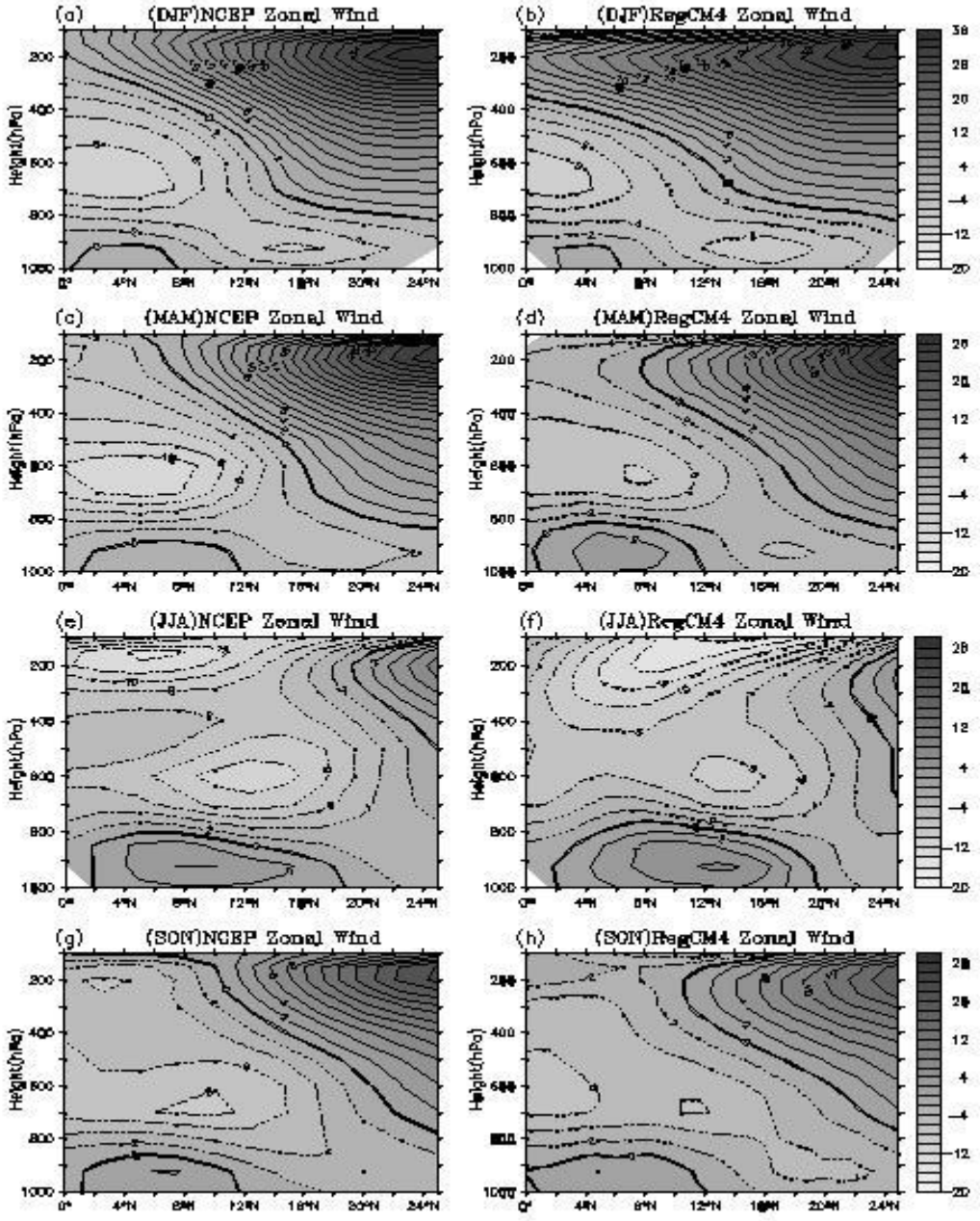

Figure 10: Vertical cross section of the zonal wind averaged between 20°E and 20°W and for the whole period of simulation (1998–2010) for NCEP (left) and RegCM4 (right) for December-February (DJF), March-May (MAM), June-August (JJA) and September-November (SON).

In SON, it is observed that intensities of the AEJ at 600 hPa and the TEJ at 200 hPa start reducing over this period. The strength of AEJ in the RegCM4 (model) is observed to be weaker by about $2ms^{-1}$ with respect to NCEP (reanalysis). At the lower levels between 1000-800 hPa, the westerlies are observed to retreat southward with the harmattan (around 22°N) appearing again over West Africa. This is related to the southward displacement of the ITCZ and thus depict the second rainy season the Guinean Coast.

Convective activity and rainfall are related to these circulation features over West Africa. The study of the relationship between the AEJ and the MCSs occurring over West Africa by Mohr and Thorncroft (2006) showed that such intense systems tend to occur more frequently north of the AEJ. Most long-lived squall lines that cross the region are observed to occur in the domain of the jet (Mathon and Laurent, 2001) and most of the precipitation in West Africa is associated with MCSs (D'Amato and Lebel, 1998), which are organized along the AEJ (Mathon and Laurent 2001).

West African summer climatology

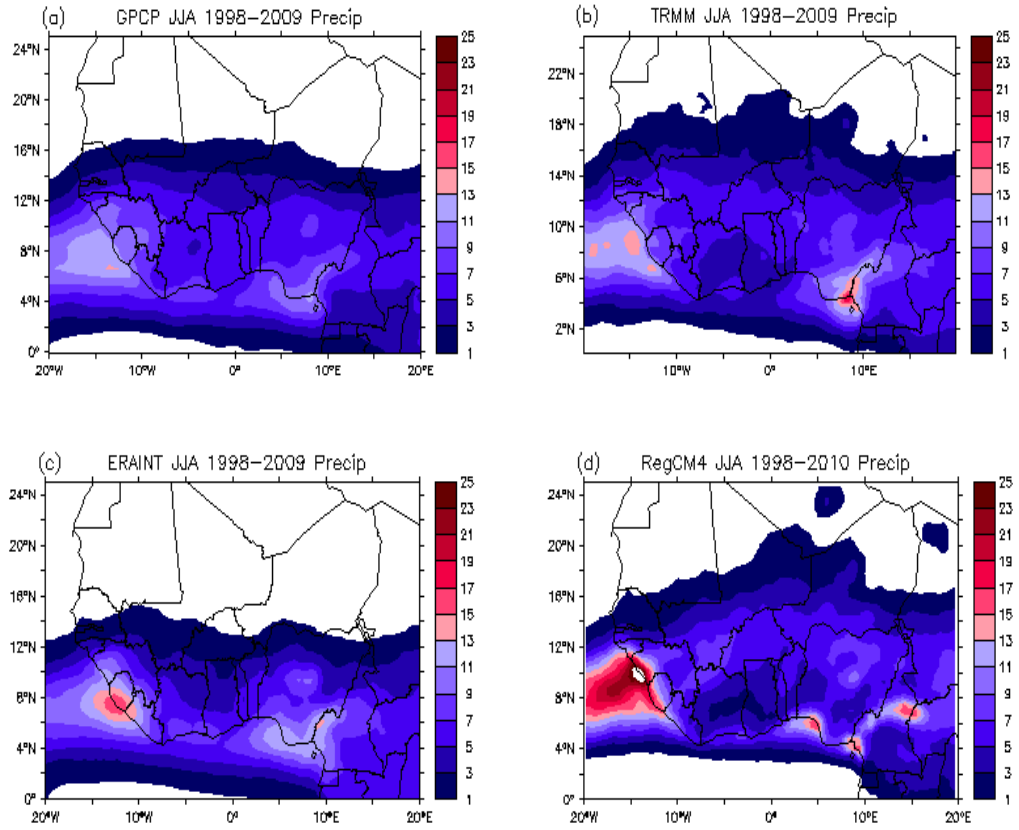

Figure 11: Averaged JJA precipitation for their whole period for (a) GPCP (1998–2009); (b) TRMM (1998–2009); (c) ERAINT (1998–2009) and (d) RegCM4 (1998–2010).

Figure 11 shows the JJA precipitation climatology from GPCP (1998–2009), TRMM (1998–2009), ERAINT (1998–2009), and RegCM4 (1998–2010) simulation, respectively. GPCP observations show maxima of summer rainfall (13 mm/day) in the Atlantic Ocean, and another maximum of over 9 mm/day encompassing the Cameroun Mountains, the Joss Plateau and regions west of it. The ITCZ is located in a thick zonal band between 4°N and 12°N and rainfall decreases northward and southward of the thick zonal ITCZ band up to 16°N and

1°N respectively. The TRMM dataset captures the maximum in the Atlantic Ocean around 15 mm/day also capture those over the Cameroun Mountains and Joss Plateau of about 13mm/day. It shows some fine scale localized high rainfall amount features that may be related to the local topography in the position of the ITCZ in a zonal band between 6°N and 13°N. The ERAINT dataset show maxima of summer rainfall (15 mm/day) over orographic zones of the Guinea Highlands, extending westward, and another maximum of 11mm/day over the Cameroun Mountains, encompassing the Joss Plateau and regions west of it. The ICTZ is located in a zonal band between 4°N and 11°N.

The regional model (RegCM4) simulates well the ITCZ in rainfall amounts with a maximum of about 21mm/day over the Guinea Highlands and extending into the Atlantic Ocean. It also shows a number of fine scale features related to the local topography in good agreement with the TRMM data in the region of the Cameroon Mountains and Jos Plateau which are not present in the much coarse resolution GPCP dataset. Zonal rainfall gradients over both sides of the ITCZ are well captured.

In general, precipitation decreases south and north of the maximum rainbelt. The monsoon rainbelt is more sharply defined in RegCM4 and TRMM than in the GPCP and ERAINT datasets. This might possibly be related to the high resolution of the regional model and the TRMM data with respect to that of GPCP and ERAINT datasets. The issue of discrepancies across different observed rainfall climatologies has been discussed extensively by Sylla *et al*. (2009a). This analysis is a confirmation to the fact that significant uncertainties are present in

observed precipitation climatologies and the RegCM4 precipitation is within the range of these uncertainties. The underestimation of rainfall amount over highlands may be linked to the failure of observation datasets to resolve topography accurately. Similar underestimations in rainfall amount have been observed in regional model simulations over West Africa and East Africa (Jenkins, 1997 and Sun *et al*., 1999). Afiesimama *et al*. (2006) suggests that the underestimated rainfall may be related to the choice of convection scheme used. Overall, the rainfall pattern is well captured by RegCM4.

It is noticed, however, that in JJA, the ITCZ is located at its northernmost position and the West African monsoon rainfall is at its maximum. This precipitation is mainly associated with the frequent occurrence of propagating MCSs related to the dynamics of the AEJ and TEJ (Jenkins *et al*. 2005; D'Amato and Lebel 1998).

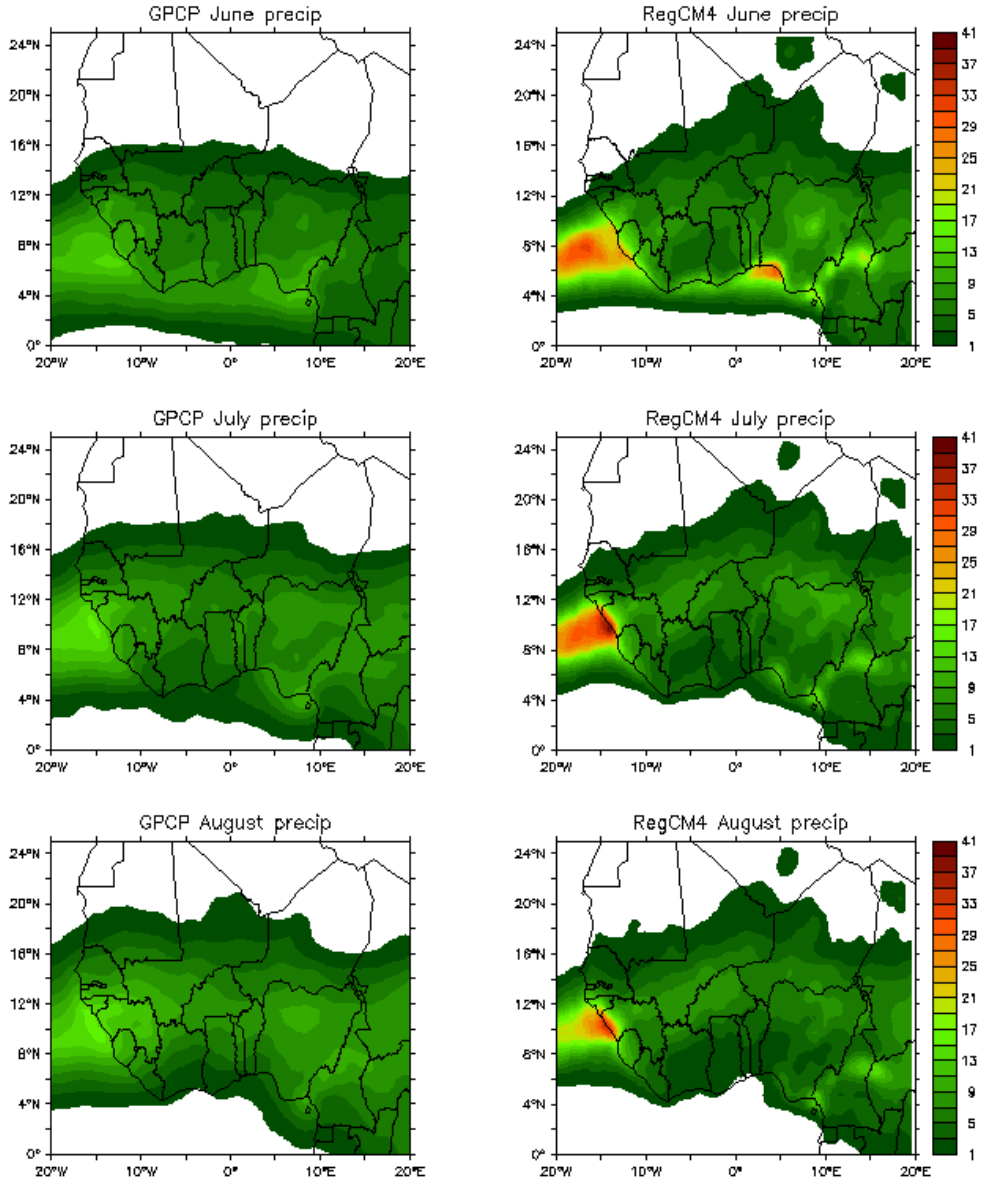

Figure 12: Month-to-month variability of averaged rainfall (1998–2010) from GPCP (left panels) and RegCM4 (right panels) in June (upper panels), July (middle panels), and August (lower panels).

We observe the month-to-month rainfall variability during JJA and its possible connection with the AEJ, TEJ and convection. For precipitation, the coarse resolution GPCP observations are used here to compare to the regional model (1998–2010). Figure 12 shows the monthly rainfall from GPCP (left panels) and RegCM4 (right panels) for June (upper), July (middle), and August (lower). In June, intense observed rainfall is mostly located along the Gulf of Guinea. RegCM4 reproduces the high precipitation over the Gulf of Guinea and overestimate the precipitation observed in GPCP. In July, both the observations and model move the rain band core up to 11–12 °N, leaving the Gulf of Guinea drier. In August, the rain band is at its northernmost location around 14°N, with a good agreement between GPCP and RegCM4 (Figure 12).

Temporal variability of West African climate

In this section, we examine the time-latitude cross sections, from 0° to 25°N, of annual cycle of rainfall averaged between 20°W and 20°E for TRMM, GPCP and RegCM4 datasets for the period of simulations, 1998 – 2010. Figure 13 shows the time-latitude cross section of the mean annual rainfall superimposed with mean 925 hPa horizontal wind field. The vectors clearly show the moist southwesterly trade winds (monsoonal winds) from the Gulf of Guinea and the dry northeasterly trade winds from the Sahara desert. The boundary between these two air masses of different origins forms the low pressure zone known as the ITCZ.

As shown in Figure 13, three sets of rainfall maxima associated with the latitudinal location of the ITCZ are observed in the annual cycle. The first phase of rainfall appear in April and runs through to October in GPCP (Fig. 13a), early May to late June in TRMM (Fig. 13b) and early March to late May in RegCM4 (Fig. 13c). The second is in July to late August in both GPCP and TRMM (Fig. 13a, b) and early June to August in RegCM4 (Fig. 13c). The third appears only in RegCM4 and occurs in early September and runs through to late October. The coastal regions, south of 8°N are distinguished by two rainy season regimes, while regions north of 10°N are distinguished by a single rainy season regime. Studies have proven that the evolution of West African monsoon rainfall is distinguished by three distinct phases (Le Barbé *et al*., 2002; Sultan and Janicot, 2003b; Zhang *et al*., 2006). Constant with these studies, the features displayed in Figure 13 can be classified into onset, intensification and cessation phases respectively, where the cessation in RegCM4 is much intense than it does in the GPCP and TRMM results.

The onset phase, from both GPCP and TRMM, begins in March to late June (Fig. 13a, b), while in RegCM4, it starts from February to early May (Fig. 13c). The onset phase is distinguished by rain band intensification along the Guinean Coast. The ITCZ is located between the equator and 8°N by this time. During July to late August in both GPCP and TRMM, and June to late August in RegCM4, maximum rainfall which marks the second phase is observed. During this period, a sudden northward shift (referred to as 'monsoon jump') in the rainbelt into the Sahel region of West Africa occurs, consistent with the

northernmost position of the ITCZ. The rainbelt at this time is located between 9° and 12°N in both GPCP and TRMM. The RegCM4 captures well the monsoon jump and the rainbelt is well simulated, but it is located farther north between 10° and 16°N. The changes in the rainfall band marked the beginning of intensified rainy season in the Sahel (Camberlin and Diop, 2003); with evidence of sudden discontinuity of heavy rainfall along the Guinean coast. Preceding studies such as Adedokun, (1978) and Omotosho (1988) have proven that the reduction in rainfall along the Guinean Coast region, associated with the alleged little dry season from July to mid-September, is not connected to lack of moisture in the atmosphere. It is known that during this period, monsoon is fully developed (Sultan and Janicot, 2003b), which suggests the abundance of moisture in the atmosphere. Omotosho (1988) suggested that the lower rainfall is due to the stronger subsidence associated with outflows from deep convective systems located to the north of the area.

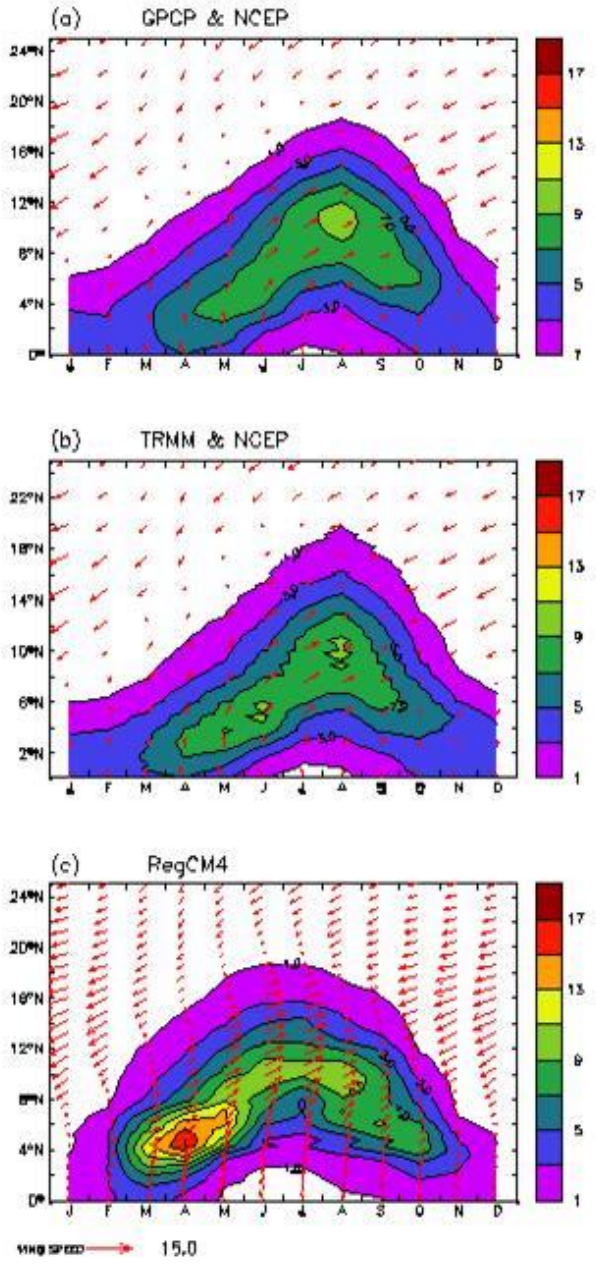

Figure 13: The time-latitude cross-section of mean rainfall averaged between 20°W and 20°E for (a) GPCP, (b) TRMM, and (c) RegCM4 for 1998–2010. The NCEP 925hPa wind field shown in vectors (arrows) is superimposed on the GPCP and TRMM rainfall. The model's 925 hPa wind field shown also in vectors is superimposed on its mean rainfall. The vector scale in ms^{-1} is shown at the bottom of the panels.

The final phase of the WAM rainfall is followed by the cessation phase beginning from October (Le Barbé *et al*., 2002; Camberlin and Diop, 2003) to late February. During this period, rainfall amount decreases and gradually retreats southwards to its southernmost position at the coast, consistent with the southernmost position of the ITCZ. During this phase, the ITCZ lies between the equator and 8°N. The three phases are closely linked to (i) the position and northward movement of the ITCZ, (ii) the peak in mesoscale convection and (iii) the southward retreat of the ITCZ.

Mean winds at 600 and 200 hPa

The mean wind field at 600 hPa (Figures 14) over West Africa shows the location and intensity of the AEJ in June-August in NCEP and RegCM4. The NCEP wind field at 600 hPa locates the core of the AEJ around 12°N in June (Figure 14(a)) exceeding 12 m/s over a large zonal band. In July (Figure 14(c)), the jet core is narrower and is located at 15°N, while in August (Figure 14(e)), it is found around 17°N. The AEJ is observed to undergo a northward migration as it becomes weaker throughout the summer season. During the summer season, from June, when the AEJ is at its southernmost mean latitudinal position, to August, at its northernmost latitudinal position, AEJ moves northwards at a regular latitudinal interval of about 2° per month.

The RegCM4 model (Figure 14(d) and (f)) follows fairly well that of the reanalysis but simulates a somewhat weaker AEJ as compared to NCEP. It shows the jet core at the same latitudes as the reanalysis in June (12°N) with speed of

about 11 ms^{-1}, July (15°N) at 10 ms^{-1}, and August (17°N) at 10 ms^{-1} which shows an underestimation of its speed of about 2 ms^{-1}. Since the position of AEJ has a link with seasonal rainfall variability, it proposes that part of the underestimation of rainfall over Guinean Coast may be due to the northward extent of the jet.

The mean wind shear at 200 hPa (Figure 15) over West Africa shows the monthly magnitude and location of the TEJ for three summer months of June, July and August for NCEP and RegCM4. In the upper levels of the troposphere, the TEJ from the reanalysis starts drifting over West Africa in June (Figure 15(a)). It is observed June that the TEJ peaks around 10 ms^{-1} at 5°N in June, around 16 ms^{-1} at 7°N in July, also around 17 ms^{-1} at 5°N in August. The area covered by the core becomes wider in July and August (Figure 15(c) and (e)) while there was an increase in its strength through the region. The TEJ gets to its maximum intensity in July/August and is at its northernmost position in July. In August, the TEJ begins to shift southward as seen in Figure 15e during the period of this study. The jet weakens as it moves southwards.

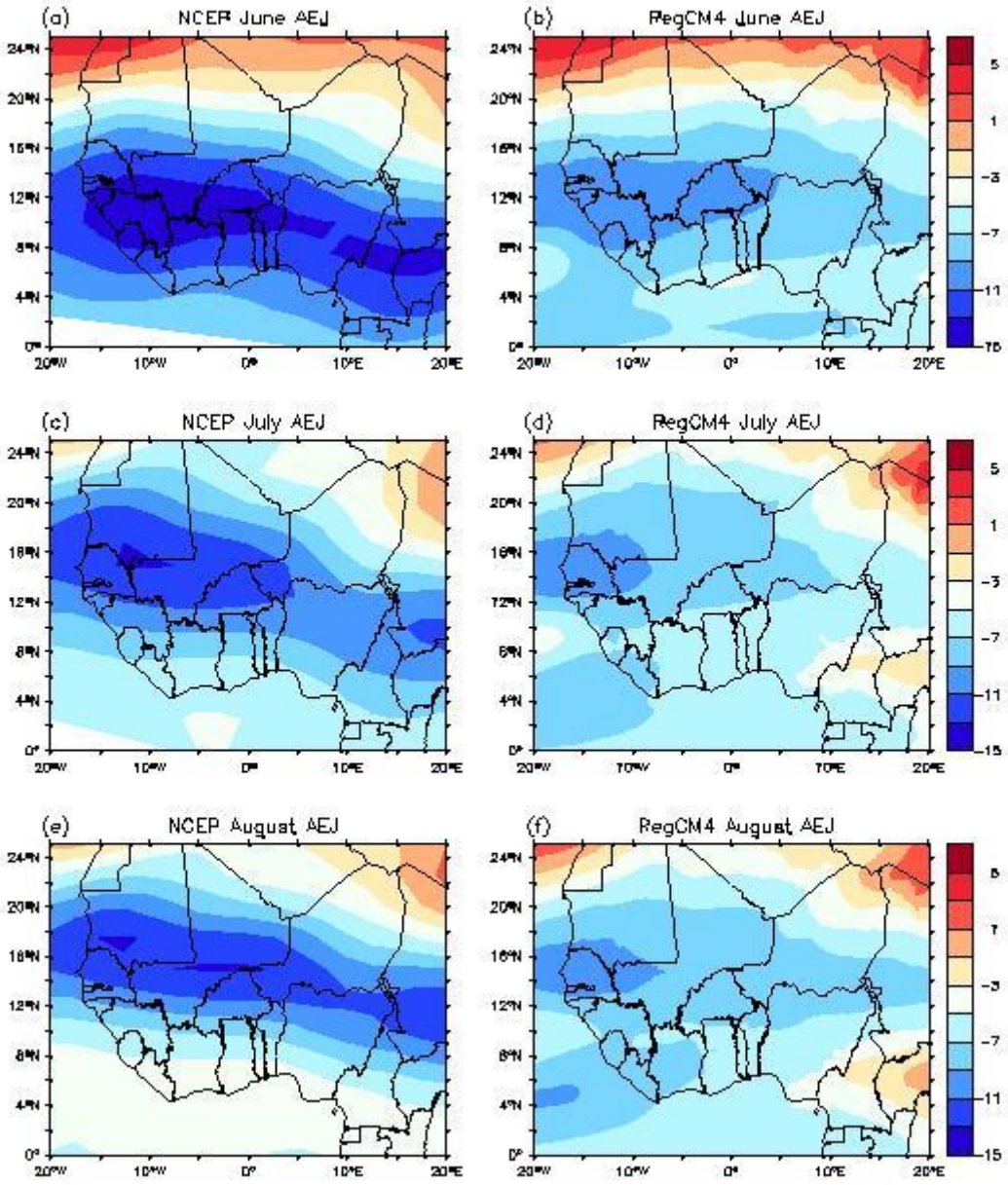

Figure 14: Month-to-month variability of averaged 600 hPa zonal wind (1998–2010) from NCEP (left panels) and RegCM4 (right panels) in June (upper panels), July (middle panels), and August (lower panels).

The RegCM4 model, in comparison to the NCEP (Figure 15(b), (d) and (f)) captures all the monthly changes as the reanalysis, but there is also an overestimation of the core speed of the TEJ by about 2 ms^{-1}. RegCM4 produces core speeds of 12 ms^{-1} at 8°N (June), 19 ms^{-1} at 9°N (July), 20 ms^{-1} at 8°N (August). The existence of this jet proposes that there is a layer of warmer air to the north and cooler air to the south of the jet. Studies have proven that the jet is being driven by the differential heating and cooling that exist between the Tibetan highlands and the Indian Ocean (Nicholson and Grist, 2003). The difference in the latitudinal position of about 3° north in RegCM4 and NCEP could have a significant impact on the simulated rainfall over West Africa, as studies have shown that TEJ plays important roles in West African rainfall (Jenkins *et al*, 2005; Nicholson, 2009).

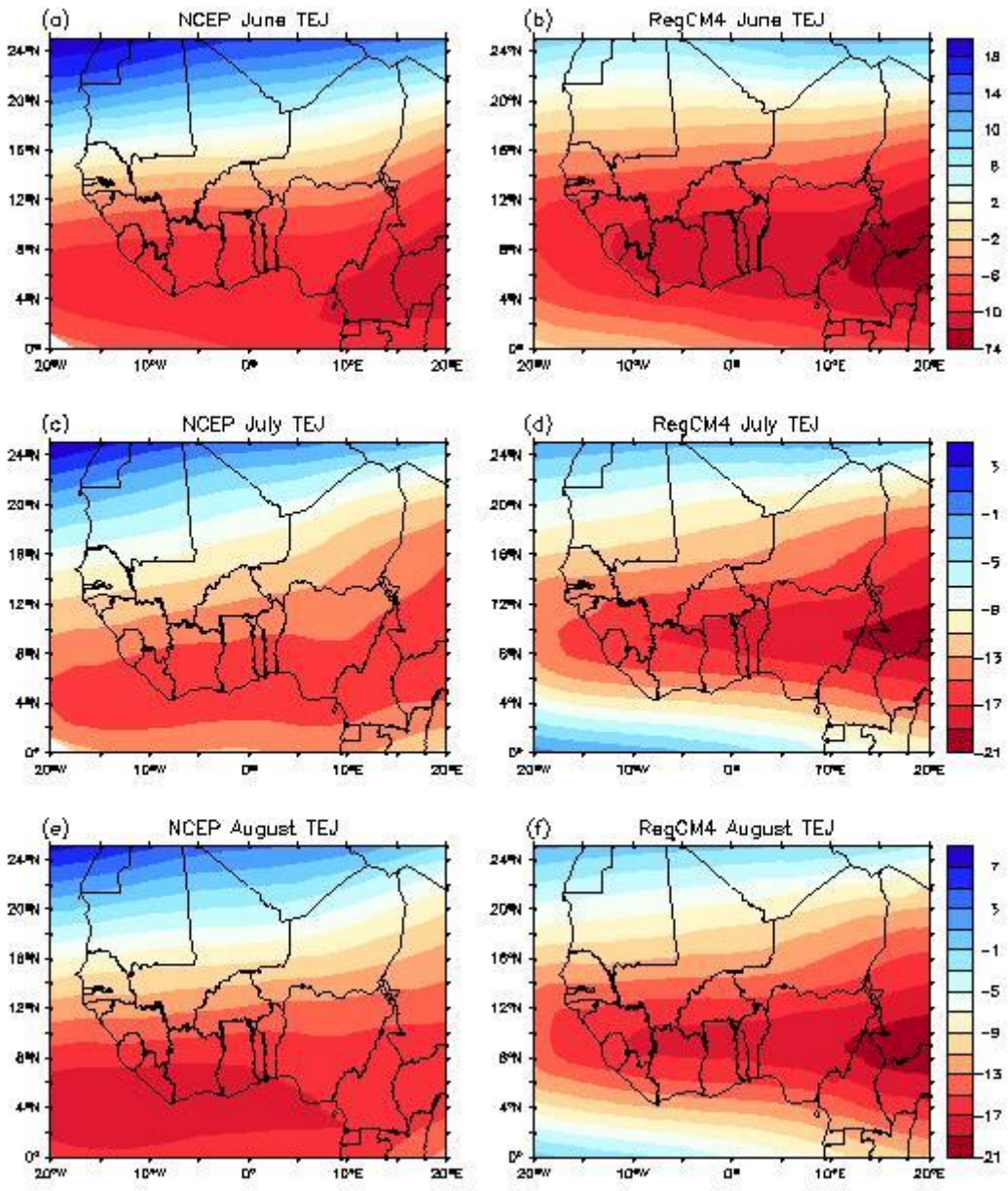

Figure 15: Month-to-month variability of averaged 200 hPa zonal wind (1998–2010) from NCEP (left panels) and RegCM4 (right panels) in June (upper panels), July (middle panels), and August (lower panels).

Monthly rainfall variability study

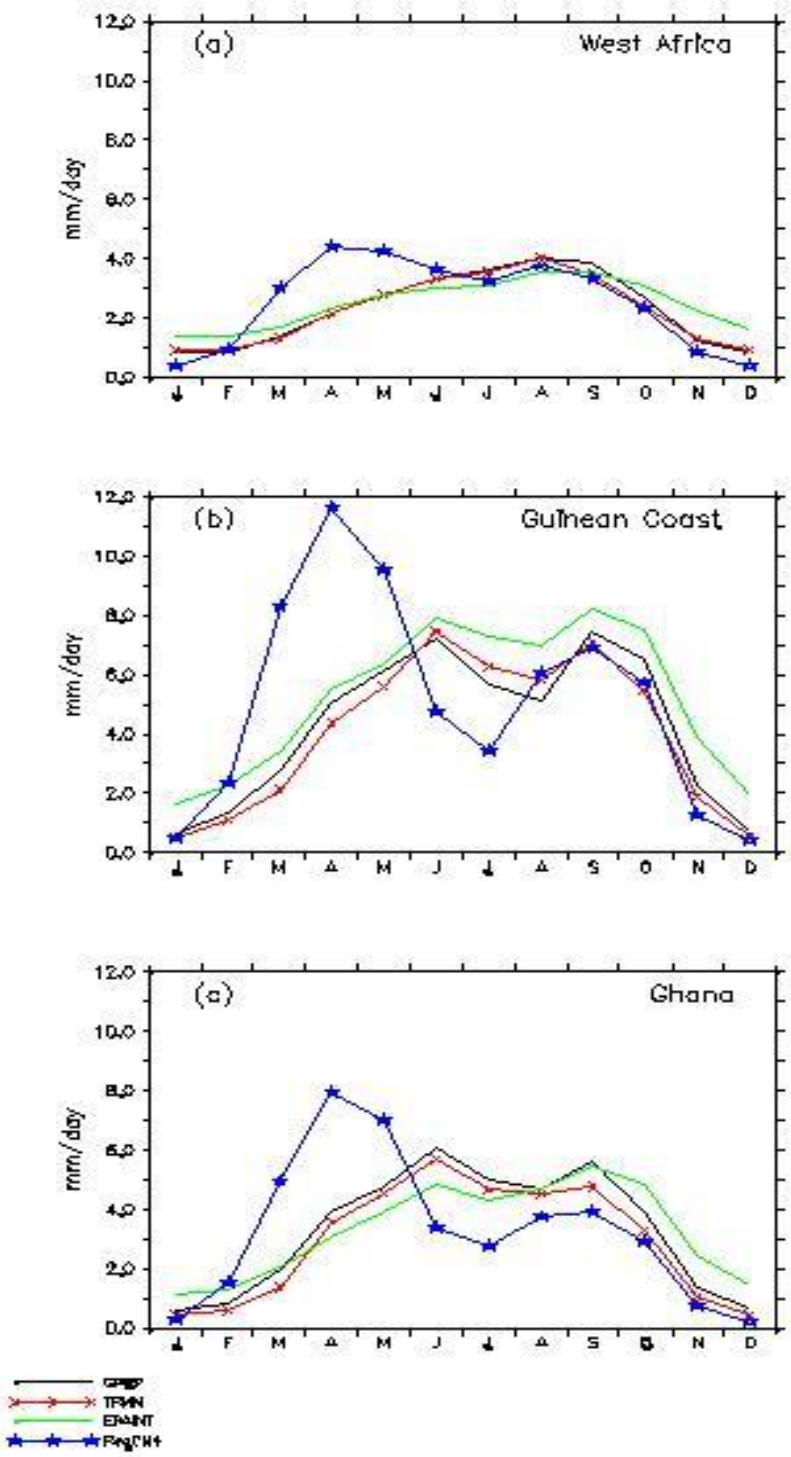

Figure 16: Monthly mean precipitation (mm/day) patterns over West Africa, the Guinean Coast and Ghana for 1998-2010.

For precipitation, the observations (GPCP and TRMM) and reanalysis (ERAINT) show a bell-shaped pattern with its peak in August over West Africa (Fig. 16a). The model (RegCM4) has two peaks, one in April/May and the second in August. The model's second peak agrees well in both amount and position with that of the observations (GPCP and TRMM) and reanalysis (ERAINT). It is well observed that the model overestimates rainfall in the March/April/May (MAM) period over the whole West Africa. Observations made during the retreating of the monsoon in October and November showed an overestimation of about 0.5 mm/day of rainfall in the reanalysis (ERAINT) and an underestimation of about 0.5 mm/day of rainfall in the model (RegCM4).

Due to the location of Ghana in the West African region, the domain is reduced for analysis over the Guinean Coast to demonstrate variations in precipitation that might as well take place over Ghana. (Figure 16b). The Guinean Coast has two peaks, one in June and the other in September, with minimum rainfall in August (Figure 16b). Adefolalu (1974), Adegoke and Lamptey (2000) discussed that the rainfall minimum that occur in August might likely be connected to the relative stability that exist over the coastal area as a result of lower sea surface temperature and the divergence of specific humidity during the period. The model is observed to have its minimum rainfall in July and its maximum first peak in April, whereas its second peak is well stimulated to agree with the observation and reanalysis. A dry spell is observed from November to February in the year. It is observed also that the model accurately stimulated the

dry seasons in the year although there is a tendency for the model to overestimate rainfall in the Guinean Coast due to its complex climate variability.

In Figure 16c, Ghana is observed to have the same precipitation trend as that of the Guinean Coast, but with lower intensities in all datasets being analyzed. The model in Figure 16b overestimates the rainfall intensity over the MAM period but virtually underestimates the amount of rains for the rest of the year. The lower intensity in rainfall over Ghana in comparison to that over the Guinean Coast might be due to the mixed sub-region nature of Ghana, with the northernmost part of the country located in the Central Soudano-Sahel region of West Africa.

Linear association between SSTs and Rainfall over West Africa

The atmosphere, land and the ocean are very much connected. The temperatures experienced over the ocean have influence on rainfall patterns throughout the world, so when there is a change in the ocean temperatures, rainfall patterns are expected to change as well. In figure 17a, a high negative correlation is observed over Guinea, Sierra Leone, and part of Mali and Senegal. This negative correlation is also observed in figure 17c over a smaller region than in 17a. Over Nigeria, figure 17c recorded a negative correlation in JJA. The negative correlation depicts dry (wet) rainfall season when the temperatures over the Atlantic are warm (cold). The model, RegCM4, is observed to show a good representation of positive correlation over most part of the coast as also observed in GPCP and TRMM. In general, it is observed that SST's and rainfall show a

positive correlation over the Guinean Coast than other part of the West African region. High temperatures over the Atlantic Ocean are therefore associated with high rainfall in JJA over the Guinean Coast. Over Ghana, good positive correlation is observed, depicting high temperatures during the rainy season. Rainfall variability in Ghana is therefore seen to be much influenced by SSTs due to its position along coast of the Atlantic Ocean.

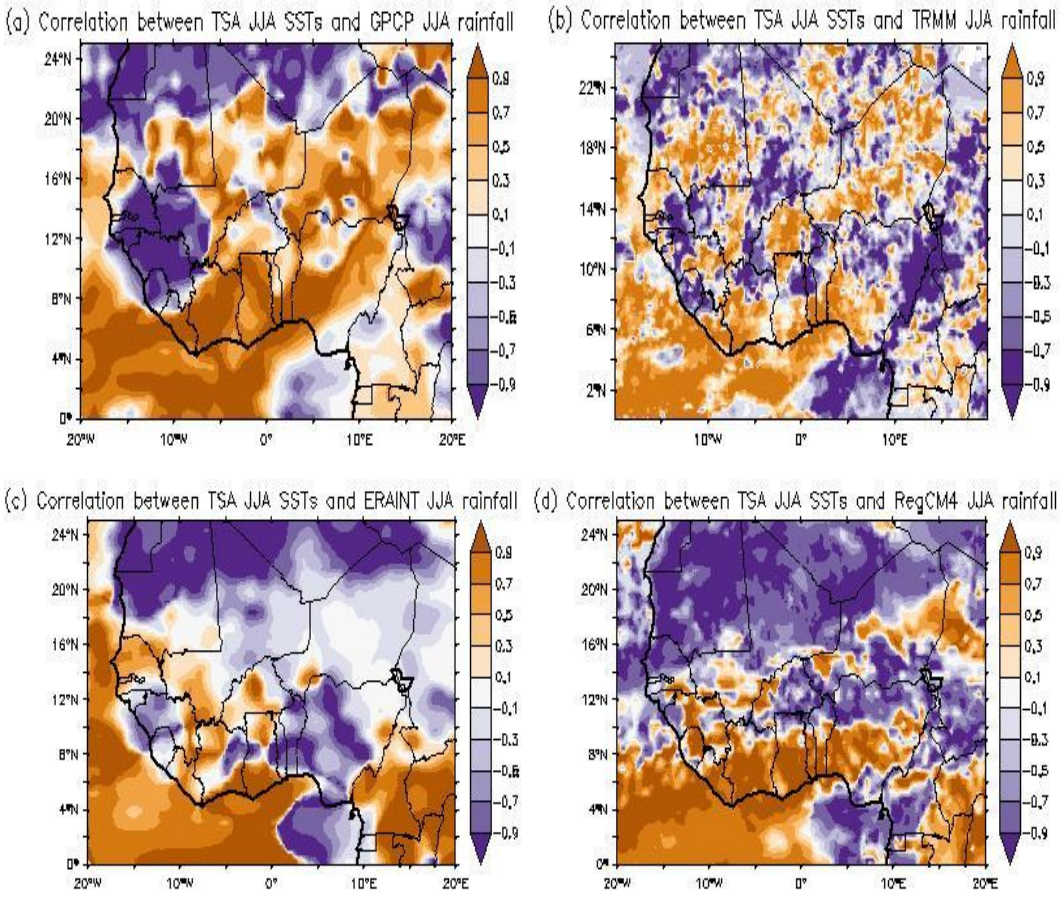

Figure 17: (a) Observed correlation between rainfall (GPCP), (b) TRMM, (c) ERAINT and local SST (TSA) for June-July-August and (d) simulated rainfall (RegCM4) correlation with local SST (TSA) for June-July-August over West Africa.

One important observation made is the possibility of forecasting rainfall over Ghana using the correlation between SSTs and rainfall amounts three months later. Since SSTs influence rainfall over the coast of West Africa, they provide a strong basis to how rainfall will behave in the next few months. An observation of the correlation between the March-April-May (MAM) SSTs and June-July-August (JJA) rainfall over coast of Ghana show a positive correlation in GPCP (Figure 18). A positive correlation is observed in the middle belt of Ghana in TRMM, and strongly over the north of Ghana in ERAINT. The simulated data, RegCM4, records slight positive correlation at the very west of the country. It can be observed from this analysis that the knowledge of SSTs in the MAM period can provide suggestions of how rainfall will behave in the JJA period although the correlation is not so strong as compared to the bi-monthly lag correlation observed by Opoku-Ankomah and Cordrey (1994).

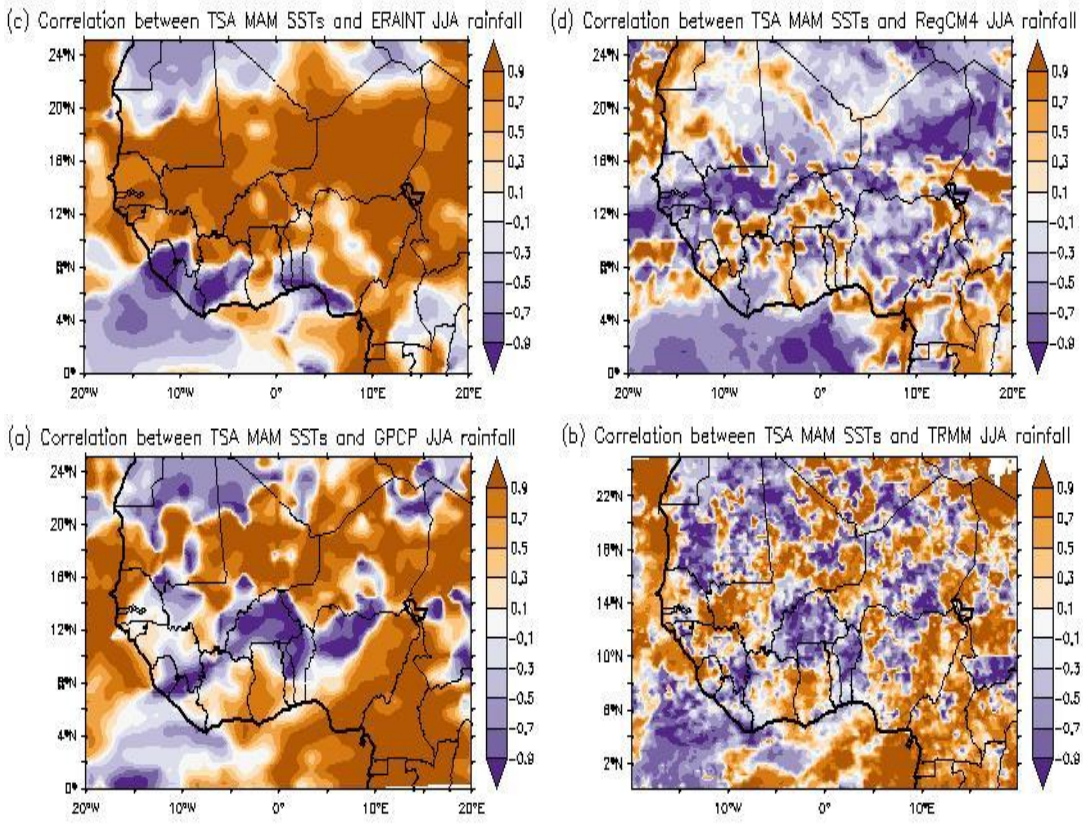

Figure 18: (a) Observed correlation between rainfall (GPCP), (b) TRMM, (c) ERAINT, (d) simulated rainfall (RegCM4) for June-July-August and local SST (TSA) for March-April-May over West Africa.

Seasonal Rainfall Variability in Ghana

Due to the complex nature of Ghana's spatial climate variability (Cooper *et al*, 2008), with the coexistence of different precipitation regimes from the wet Guinean Coast to the dry Sahelian region, different patterns in rainfall amount over various parts of the country were observed. It was observed that the northern belt of the country has a uni-modal rainfall distribution type which starts from March to October with August recording the highest amount of rainfall of 243 mm (Figure 19). March, which is the start of the rainfall period over the northern

belt records rainfall amount of 15 mm with October recording 80 mm of rainfall as the cessation of rainfall over this region. This has been the general rainfall pattern in northern Ghana (see Figure 3) and since the maximum rainfall occurs once in a year, the pattern can be referred to as having a uni-modal rainfall distribution.

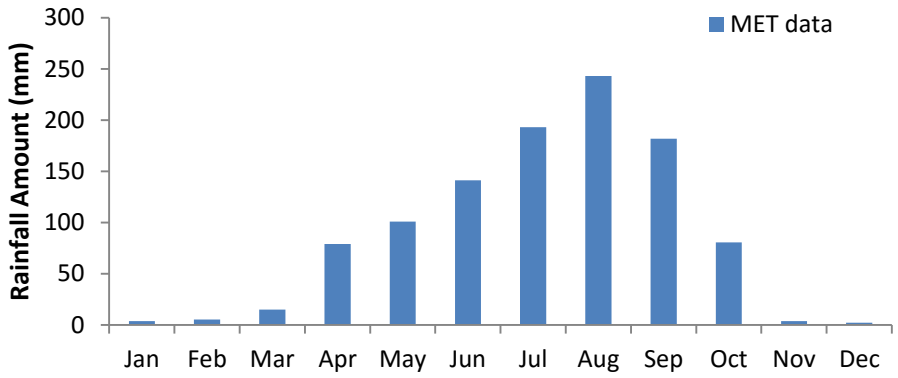

Figure 19: Average monthly rainfall variability over the northern belt of Ghana for the period 1998-2010

The part of Ghana which is located at the middle belt observe a bi-modal rainfall distribution of almost equal peaks and also exhibit similarities in the nature of their rainfall patterns with lower amount of rainfall in August separating the two peaks (Figure 20). Rainfall over this region starts around March and ends around November. Its first rainfall maximum is recorded in June with a rainfall amount of 185 mm and a second maximum of 185 mm also recorded in October.

The southern belt of Ghana also exhibits a bi-modal rainfall distribution type but have its first peak higher than the second, with August recording a lower rainfall amount to separate the two peaks (Figure 21). A first average rainfall

maximum of 202 mm is recorded in June. There is also a relatively short minor season in this region (secondary peak) from September to mid of November, with October recording the second maximum of 70 mm, when the ITCZ retreats back to the coast.

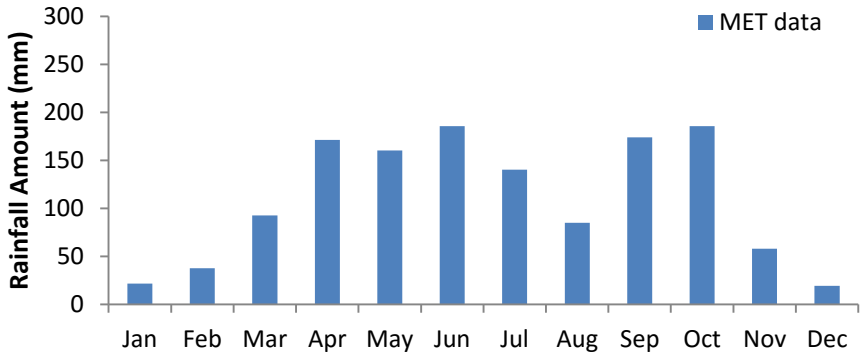

Figure 20: Average monthly rainfall variability over the middle belt of Ghana for the period 1998-2010

These rainfall patterns account for the one farming season in northern Ghana and two in the middle and southern parts of Ghana (see Figure 3). Past studies have shown that these climatic zones are strongly influenced by the movement of the Inter-Tropical Convergence Zone (ITCZ), which is responsible for both rainfall regimes (Sultan *et al*. 2005, Rodgers *et al*. 2007). The differences in the variability of rainfall in Ghana, as suggested in the national study of Opoku-Ankomah and Cordrey (1994), is due to the movement of ITCZ and influence of Atlantic SSTs of the Guinea coast, as noted by Boateng (1967). The northward and southward movement of the ITCZ over Ghana, by Sultan and

Janicot (2003) gives rise to the uni- and bi-modal regimes that characterize the northern and southern parts of the country, respectively. Analysis of the regions with the two peaks (the middle belt and southern belt), the first around May/June and a second in September/October, saw a relative minimum rainfall in August (Figures 20-21). This rainfall minimum in August, by Adefolalu (1974), and Adegoke and Lamptey (2000), is likely connected with the relative stability that exists over the coastal area as a result of lower sea surface temperature and divergence of specific humidity during this period.

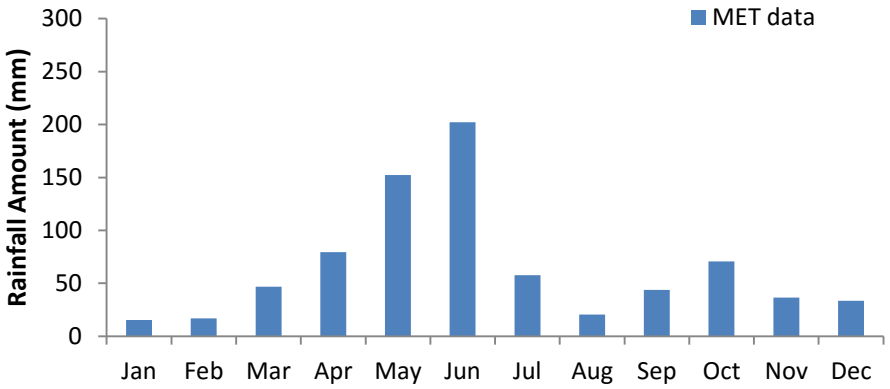

Figure 21: Average monthly rainfall variability over the southern belt of Ghana for the period 1998-2010

CHAPTER FIVE

CONCLUSIONS

The intraseasonal variability of the West African rainfall and its related large-scale dynamics has been well described from the view of simulation and observations. A regional climate model, RegCM4, which is driven at the lateral boundaries by fields from the ERA-Interim reanalysis, the most recent and improved reanalysis product available, to examine the intraseasonal rainfall variability of the West African climate was used. A comparison of the RegCM4 rainfall with GPCP, TRMM and ERAINT datasets, and the atmospheric circulations are compared with NCEP. The focus of this study is to investigate the dynamics of the WAM circulation and the effect of its variabilities over Ghana by simulating the spatiotemporal variability of rainfall and associated atmospheric features over West Africa. The analysis of the 13-year simulation (1998-2010) shows that the West African summer mean climate variability compared well with observations.

Aspects of the RegCM4 rainfall for West Africa are practically simulated. The model simulates the mean rainfall variability at the peak of the West African summer rainy season (June–August), and it reproduces the rainbelt associated with the ITCZ, although it locates the rainbelt farther north than that of GPCP, TRMM and ERAINT. Furthermore, RegCM4 reproduces rainfall over highland regions, but tends to overestimate the rainfall maxima over the Guinea Highlands. The intraseasonal variability of rainfall averaged over 20°W to 20°E is very well represented (Figure 11). In consistency with past studies (Sultan and Janicot,

2003b; Zhang *et al*., 2006), and consistent with GPCP and TRMM, the model captures the three easily distinguishable phases (onset, intensification and cessation phases) of the West African monsoon rainfall. The onset phase is simulated earlier, starting from early February to early May, as compared to the observations with an onset in March to late June. The RegCM4 does well in capturing the monsoon jump during the intensification phase, but moves it more northward; between 10° and 16°N compared to9° and 12°N in both GPCP and TRMM. The monthly development of rainfall demonstrates an upward-downward migration of the rainbelt reaching its northernmost position in August over the Sahel, agreeing with the northernmost limit of the ITCZ (Figure 13). The monsoon jump (abrupt shift of the rainbelt) is clearly captured by the model but it occurs in May, a bit earlier compared to GPCP and TRMM observations. These developments in the positioning and movements of the rainbelt are well demonstrated in the seasonal rainfall variability over Ghana. It is observed that the northern belt of Ghana records its rainfall maximum in August (Fig. 18). This is due to the positioning of northern Ghana in the Sahel region. The middle and southern belts of Ghana demonstrates the onset and cessation phases of the West African monsoon rainfall with both first and second maxima in June and October respectively (Figures 19 and 20).

The vertical structure of zonal wind component over the period 1998-2010 after the simulation did compare well with NCEP. The AEJ becomes weaker as it moves northward. Previous studies (e.g., Sylla *et al*., 2010) also confirmed that the monthly migration of the rainbelt, as discussed earlier, is correlated with the

weakening and northward shift of the AEJ and the emergence and strengthening of the TEJ. Also, other earlier studies agreed to the fact that the variability in the AEJ and TEJ has great influence in the variability of rainfall over West Africa (Grist and Nicholson, 2001; Patricola and Cook, 2010b). In this thesis, it was observed that the core of the rainbelt lie between the two jets, suggesting that any instability in the AEJ may lead to rainfall variability over West Africa. The correlation in the rainbelt's core and the core of the jets suggests that the vertical movement plays a significant role in rainfall.

The monthly variability of variables responsible for the rainfall variability was realistically simulated. The model captures well the monthly rainfall variability over the Guinean Coast sub-region. The rainfall pattern over the Guinean Coast which is well demonstrated by all the datasets, with an overestimation in RegCM4 and a shift in its peak, is well depicted in the rainfall pattern over Ghana. The simulation well depicts the bimodal nature of rainfall over southern Ghana. The lower intensity in rainfall over Ghana in comparison to that over the Guinean Coast is due to the mixed sub-region nature of Ghana, with the northernmost part of the country located in the Central Soudano-Sahel region of West Africa. The entire West Africa was well represented by the model with the exception of its overestimation of rainfall intensity in the MAM period. This overestimation may be due to the higher spatial resolution of the RegCM4 as compared to GPCP, TRMM AND ERAINT.

A further study of the influence of the Ocean was considered. A linear association between the South Atlantic SST and West African rainfall showed a

positive high correlation over the coast of West Africa and a negative or no correlation over the Sahel region. The positive correlation signifies high rainfall amount at warm ocean temperatures, and the negative correlation denotes low (high) rainfall amount at warm (cold) ocean temperatures. One significant finding is the three months lag correlation between the March-April-May (MAM) SSTs and June-July-August (JJA) rainfall. This correlation tend to provide an idea of the forecast of rainfall for up to three months. This system might be of benefit to the small-scale farmers whose lives depend on rainfed agriculture.

Overall, this thesis assesses the dynamics of the West African Monsoon and its variability over Ghana. In assisting the representation of the monsoon dynamics, the RegCM4 simulations are used in capturing several of the observed relationships between rainfall and related atmospheric circulations; though there were some eminent disparities in the simulations. Changes in the atmospheric circulation features and rainfall variability of the West African Monsoon have an influence over the rainfall system of Ghana. The rainfall system of Ghana, which depends mainly on the WAM system, is likely to be changing depending on (a) the stability of the atmospheric circulation features and (b) the changes in Sea Surface Temperatures (SSTs). It is also observed that the RegCM4, when driven by high quality lateral boundary conditions, can bring out a good simulation of the complex dynamics of the West African monsoon and its related circulations, and the interactions these dynamics have with precipitation.

REFERENCES

Abiodun, B. J., Pal, J. S., Afiesimama, E. A., Gutowski, W. J. and Adedoyin, A. (2008). Simulation of West African monsoon using RegCM3 Part II: impacts of deforestation and desertification. *Theoretical and Applied Climatology, 93, no. 3-4,* 245–261.

Adedokun, J. A. (1978). West African precipitation and dominant atmospheric mechanisms. *Archives for meteorology, geophysics, and bioclimatology, Series A, 27,* 289–310.

Adefolalu, D. O. (1974). On Scale Interactions and the Lower Atmospheric Summer Easterly Perturbation in Tropical West Africa. Ph.D. Thesis. *The Florida State University. Tallah*, 276.

Adegoke, J. O. and Lamptey, B. L. (2000). Intraseasonal Variability of Summertime Precipitation in the Guinea Coastal Region of West Africa. *Proceedings of the Workshop on the West African Monsoon Variability and Predictability. WMO-TD No. 1003*, 115-118

Adiku, S. G. K., Mawunya, F. D., Jones, J. W. and Yangyouru, M. (2007). Can ENSO Help in Agricultural Decision-Making in Ghana? In: Sivakumar, M. V. K. and Hansen, K., Eds., *Climate Prediction and Agriculture, Springer, Berlin Heidelberg*. http://dx.doi.org/10.1007/978-3-540-44650-7_20

Afiesimama, A. E., Pal, J. S., Abiodun, B. J., Gutowski, W. J. and Adedoyin, A. (2006). Simulation of West African monsoon using the RegCM3. Part I:

model validation and interannual variability. *Theoretical and Applied Climatology, 86, no. 1–4,* 23–37.

Adler, R. F., Huffman, G. J., Chang, A., Ferraro, R., Xie, P., Janowiak, J., Rudolf, B., Schneider, U., Curtis, S., Bolvin, D., Gruber, A., Susskind, J., Arkin, P. and Nelkin, E. (2003). The version-2 global precipitation climatology project (GPCP) monthly precipitation analysis (1979-present), *Journal of Hydrometeorology, 4*, 1147-1167.

Anthes, R. A. (1977). A cumulus parameterization scheme utilizing a one-dimensional cloud model. *Monthly Weather Review*, *105*: 1423–1438

Anthes, R.A., Kuo, Y. H., Hsie, E. Y., Low-Nam, S. and Bettge, T. W. (1989). Estimation of skill and uncertainty in regional numerical models. *Quarterly Journal of the Royal Meteorological Society, 115*, 763-806.

Bader, J. and Latif, M. (2003). The impact of decadal-scale Indian Ocean sea surface temperature anomalies on Sahelian rainfall and the North Atlantic Oscillation. *Geophysical Research Letter, 30,* 2169, doi:10.1029/2003 GL018426.

Bard, E. (2002). Climate shock: Abrupt changes over millennial time scales. *Physics Today, 55 (12):* 32-38.

Baron, C., Sultan, B., Balme, M., Sarr, B., Lebel, T., Janicot, S. and Dingkuhn, M. (2005). From GCM grid cell to agricultural plot: Scale issues affecting modeling of climate impact. *Philosophical Transactions of the Royal Society of London, 360B (1463),* 2095-2108.

Boateng, E. A. (1967). A Geography of Ghana. *Cambridge University Press, Cambridge*, 212 .

Briegleb, B. P. (1992). Delta-Eddington approximation for solar radiation in the NCAR Community Climate Model. *Journal of Geophysical Research*, *97*, 7603–7612

Browne, N. A. K. and Sylla, M.B. (2012). Regional Climate Model Sensitivity to Domain Size for the Simulation of the West African Monsoon Rainfall. *International Journal of Geophysics*, *2012*, Article ID: 625831. http://dx.doi.org/10.1155/2012/625831

Burpee, R. W. (1972). The Origin and Structure of easterly waves in the lower troposphere of North Africa. *Journal of the Atmospheric Sciences, 29,* 77-90.

Burpee, R. W. (1974). Characteristics of North African Easterly Waves During the Summers of 1968 and 1969. *Journal of the Atmospheric Sciences*, *31*, 1556-1570.

Camberlin, P., and Diop, M. (2003). Application of daily rainfall principal component analysis to the assessment of the rainy season characteristics in Senegal. *Climate Research*, *23,* 159–169.

Cavalcanti, I. F. A., Pezzi, L. P., Nobre P., Sampaio G. and Camargo, Jr. H. (1998). Climate prediction of precipitation in Brazil for the Northeast raining season (MAM) 1998. *Experimental Long-Lead Forecast Bulletin, 7, No. 1,* 24-27.

Charney, J. G. and Stern, M. E. (1962). On the stability of internal baroclinic jets in a rotating atmosphere. *Journal of the Atmospheric Sciences*, *19*, 159-172.

Charney, J. G. (1973). Planetary fluid dynamics. *Dynamic Meteorology, P. Morel, Ed., D. Reidel*, 97-352.

Cook, K. H. (1999). Generation of the African Easterly Jet and Its Role is Determining West African Preciptation. *Journal of Climate*, *12***,** 1165-1184.

Cooper, P. J. M., Dimes, J., Rao, K. P. C., Shapiro, B., Shiferaw, B., Twomlow, S. (2008). Coping better with current climatic variability in the rain-fed farming systems of sub-Saharan Africa: An essential first step in adapting to future climate change? *Agriculture, Ecosystems and Environment, 126,* 24-35

D'Amato, N., and Lebel, T. (1998). On the characteristics of the rainfall events in the Sahel with a view to the analysis of climatic variability. *International Journal of Climatology*. *18*, 955-974.

Dai, A., and Trenberth, K.E. (2004). The diurnal cycle and its depiction in the community climate system model. *Journal of Climate, 17*, 930-951.

Dickinson, R. E., Henderson-Sellers, A. and Kennedy, P. (1993). Biosphere–atmosphere transfer scheme (BATS) version 1e as coupled to the NCAR community climate model. Tech Rep, National Center for Atmospheric Research Tech Note NCAR.TN-387+STR, NCAR, Boulder, CO

Diro, G. T., Rausher, S. A., Giorgi, F. and Tompkins, A. M. (2012). Sensitivity of seasonal climate and diurnal precipitation over Central America to land and sea surface schemes in RegCM4. *Climate Research, 52*, 31–48

Farmer, G. and Wigley, T.M.L. (1985). Climatic Trends for Tropical Africa, *Research Rep. for the Overseas Development Administration*, 136.

Fink, A. H. and Reiner, A. (2003). Spatiotemporal variability of the relation between African Easterly Waves and West African Squall Lines in 1998 and 1999. *Journal of Geophysical Research*, 108 (D11), 10.1029/2002 JD002816.

Folland, C. K., Owen, J. A., Ward, M. N. and Colman, A. W. (1991). Prediction of seasonal rainfall in the Sahel region using empirical and dynamical methods. *Journal of Forecasting, 10*, 21-56.

Friesen, J. (2002). Spatio-Temporal Patterns of Rainfall in Northern Ghana. *Diploma Thesis, University of Bonn*, Germany.

Gaye, A., Viltard, A. and de F´elice, P. (2005). Squall lines and rainfall over Western Africa during summer 1986 and 87. *Meteorology and Atmospheric Physics, 90, no. 3-4*, 215–224.

Giannini, A., Saravanan, R. and Chang, P. (200). Dynamics of the boreal summer African monsoon in the NSIPPI atmospheric model. *Climate Dynamics, 25***,** 517-535.

Giorgi, F. and Mearns, L. O. (1999). Introduction to special section: regional climate modeling revisited. *Journal of Geophysical Research, 104*, 6335–6352.

Giorgi, F., Bi, X. and Qian, Y. (2002). Direct radiative forcing and regional climatic effects of anthropogenic aerosols over East Asia: a regional coupled climate/chemistry-aerosol model study. *Journal of Geophysical Research*, 107, 4439.

Giorgi, F., Francisco, R. and Pal, J. S. (2003). Effects of a sub-grid scale topography and landuse scheme on surface climate and hydrology. I. Effects of temperature and water vapor disaggregation. *Journal of Hydrometeorology*, 4, 317–333

Giorgi, F., Huang, Y., Nishizawa, K. and Fu, C. (1999). A seasonal cycle simulation over eastern Asia and its sensitivity to radiative transfer and surface processes. *Journal of Geophysical Research*, 104, 6403–6423

Giorgi, F., Marinucci, M. R. and Bates, G. T. (1993a). Development of a second generation regional climate model (RegCM2). Part I: boundary-layer and radiative transfer processes. *Monthly Weather Review*, 121(10), 2794–2813.

Giorgi, F., Marinucci, M. R., Bates, G. T. and Canio, G. D. (1993b). Development of a Second-Generation Regional Climate Model (RegCM2). Part II: convective processes and assimilation of lateral boundary conditions. *Monthly Weather Review*, 121, 2814–2832.

Giorgi, F., Pal, J. S., Bi, X., Sloan, L., Elguindi, N. and Solmon, F. (2006). Introduction to the TAC special issue: the RegCNET network. *Theoretical Applied Climatology*, 86, 1–4.

Goosse, H., P.Y. Barriat, W. Lefebvre, M.F. Loutre and V. Zunz, (2010). Introduction to climate dynamics and climate modeling. *Online textbook available at http://www.climate.be/textbook.*

Grell, G. A. (1993). Prognostic evaluation of assumptions used by cumulus parameterizations. *Monthly Weather Review*, *121*, 764–787

Grell, G., Dudhia, J. and Stauffer, D. R. (1994). A description of the fifth generation Penn State/NCAR Mesoscale Model (MM5). *National Center for Atmospheric Research Tech Note NCAR/TN-398 + STR, NCAR, Boulder, CO*

Grist, J. P. (200). The Atmospheric Circulation over West Africa and Equatorial Africa. *PHD Thesis, Florida State University*.

Grist, J. P., and Nicholson, S. E. (2001). A study of the dynamic factors influencing the interannual variability of rainfall in the West African Sahel. *Journal of Climate, 14*, 1337– 1359.

Gyau-Boakye, P. and Tumbulto, J. W. (2000). The Volta lake and declining rainfall and streamflows in the Volta river basin. *Environment, Development and Sustainability, 2*, 1-10

Hall, N. M. J and Peyrille, P. (2006). Dynamics of the West African Monsoon. *Journal of Physics, IV France, 139*, 81-99.

Hamilton, R. A. and Archbold, J. W. (1994). Meteorology of Nigeria and adjacent territory. *Quarterly Journal of the Royal Meteorological Society, 71*, 231-264.

Hourdin, F, Mustat, I, Guichard, F, Ruti, P. M, & Favot, F. Pham, M. M. A., Grandpeix, J. Y., Polcher, J., Marquet, P., Boone, A., Lafore, J. P., Redelsperger, J. L., Dell' Aquilla, A., Losada Doval, T., Traore, A. K., Gallee, H. (2010). AMMA-Model intercomparison project. *Bulletin of the American Meteorology Society*, doi: BAMS2791.1.

Hsieh J. S. and Cook K. H. (2007). A study of the energetics of African easterly waves. *Journal of Atmospheric Science*, *64*, 421–440.

Hulme, M., Doherty, R., Ngara, T., New, M. and Lister, D. (2001). African climate change: 1900–2100. *Climate Research*, *17*, 145–168

Im, E. S., Coppola, E., Giorgi, F. and Bi, X. (2010). Validation of a high resolution regional climate model for the Alpine region and effects of a sub-grid scale topography and land use parameterization. *Journal of Climate, 23*, 1854–1873

IPCC, (1994). Climate Change 1994: Radiative Forcing of Climate Change and an Evaluation of the IPCC IS92 Emission Scenarios, [J.T. Houghton, L.G. MeiraFilho, J. Bruce, Hoesung Lee, B.A. Callander, E. Haites, N. Harris and K. Maskell (eds.)]. *Cambridge University Press*, *Cambridge*, UK and New York, NY, USA, 339.

IPCC, (1996). Climate Change 1995: The Science of Climate Change. Contribution of Working Group I to the Second Assessment Report of the Intergovernmental Panel on Climate Change [Houghton, J.T., L.G. MeiraFilho, B.A. Callander, N. Harris, A. Kattenberg, and K. Maskell

(eds.)]. *Cambridge University Press*, Cambridge, United Kingdom and New York, NY, USA, 572.

IPCC, (1997). IPCC Technical Paper II: An introduction to simple climate models used in the IPCC Second Assessment Report, [J.T. Houghton, L.G. Meira Filho, D.J. Griggs and K. Maskell (eds.)].

Jenkins, G. S., Gaye, A. T. and Sylla, B. (2005). Late 20th century attribution of drying trends in the Sahel from the Regional Climate Model (RegCM3). *Geophysical Research Letters, 32, no. 22*, Article ID L22705, 1–4.

Jenkins, G. S., Adamou, G. and Fongang, S. (2002). The challenges of modeling climate variability in West Africa. *Climate Change, 52,* 263-286.

Jenkins, G. (1997). The 1988 and 1990 summer season simulations for West Africa using a regional climate model. *Journal of Climate, 10***,** 1255–1272.

Jones, R. G., Murphy, J. M. and Noguer, M. (1995). Simulation of climate change over Europe using a nested regional climate model I: assessment of control climate, including sensitivity to location of lateral boundary conditions. *Quarterly Journal of the Royal Meteorology Society, 121,* 1413-1449.

Kalnay, E., Kanamitsuand, M., Kistler, R., Collins, W., Deaven, D., Gandin, L., Iredell, M., Saha, S., WHite, G., Woollen, J., Zhu, Y., Chelliah, M., Ebisuzaki, W., Higgins, W., Janoeiah, J., Mo, K. C., Ropelewski, C., Wang, J., Leetmaa, A., Jenne, R. and Jeseph, D. (1996). The NCEP/NCAR 40-year reanalysis project. *Bulletin of the American Meteorological Society, 77(2),* 437–471.

Kanamitsu, M., and Krishnamurti, T. N. (1978). Northern summer tropical circulations during drought and normal rainfall months. *Monthly Weather Review*, *106*, 331–347.

Kiehl, J., Hack, J., Bonan, G., Boville, B., Breigleb, B., Williamson, D. and Rasch, P. (1996). Description of the NCAR Community Climate Model (CCM3). National Center for Atmospheric Research Tech Note NCAR/TN-420+STR, NCAR, Boulder, CO

Kiehl, J.T., and V. Ramanathan (eds.), (2006). Frontiers of Climate Modeling. *Cambridge University Press*, 367.

Kueppers, L. M., Snyder, M. A., Sloan, L. C., Cayan, D. and others (2008). Seasonal temperature response to land-use change in the western United States. *Global Planet Change*, *60*, 250–264

Lafore, J. P. and Moncrieff, M. W. (1989) A numerical investigation of organization and interaction of the convective and mesoscale region of a tropical squall line. *Journal of Atmospheric Sciences*, *46*, 521-544.

Laurent, H., Lebel, T. and Polcher, J. (1997) Rainfall variability in Soudano-Sahelian Africa studied from rain gauges, satellite and GCM. Preprints, 13th Conf. on Hydrology, Long Beach, CA, *American Meteorological Society*, 17-20.

Le Barbé, L., Lebel, T. and Tapsoba, D. (2002). Rainfall variability in West Africa during the years 1950–1990. *Journal of Climate*, *15*, 187–202.

Leroux, M. (2001). The Meteorology and Climate of Tropical Africa. *Praxis Publishing: Chichester.*

Mathon, V. and Laurent, H. (2001). Life cycle of the Sahelian mesoscale convective cloud systems. *Quarterly Journal of the Royal Meteorological Society*, *127*, 377-406.

Mathon, V., Laurent, H., and Lebel, T. (2002). Mesoscale Convective System Rainfall in the Sahel. *Journal of Applied Meteorology*, *41*, 1081-1092.

McSweeney, C., Lizcano, G., New, M. and Lu, X. (2010). The UNDP Climate Change Country Profiles. http://journals.ametsoc.org/doi/abs/ 10.1175/ 2009BAMS2826.1

Meehl, G. A., Arblaster, J. M., Lawrence, D. M., Seth, A. and Min, D. (2006). Monsoon Regimes in the CCSM3. *Journal of Climate*, *19*, 2482-2495.

Mitchell, K. E., Lohmann, D., Houser, P. R., Wood, E. F., Schaake, J. C., Robock, A., Cosgrove, B. A., Sheffield, J., Duan, Q., Luo, L., Higgins, R. W., Pinker, R. T., Tarpley, J. D., Lettenmaier, D. P., Marshall, C. H., Entin, J. K., Pan, M., Shi, W., Koren, V., Meng, J., Ramsay, B. H. and Bailey, A. A. (2004). The multi institution North American Land Data Assimilation System (NLDAS): Utilizing multiple GCIP products and partners in a continental distributed hydrological modeling system, *Journal of Geophysical Research*, 109, D07S90, doi: 10.1029/2003JD003823.

Mo, R., Fyfe, J. and Derome, J. (1998). Phase-locked and asymmetric correlations of the winter time atmospheric patters with ENSO. *Atmosphere-Ocean*, *36*, 213-239.

Mohr, K. I. and Thorncroft, C. D. (2006). Intense convective systems in West Africa and their relationship to the African easterly jet. *Quarterly Journal of the Royal Meteorological Society*, *132(614)*, 163–176.

Moufouma-Okia, W. and Rowell, D. P. (2010). Impact of soil moisture initialization and lateral boundary conditions on regional climate model simulations of the West African Monsoon. *Climate Dynamics*, *35(1)*, 213–229

Ndiaye, O., Ward, M.N., Thiaw, W.M. (2011). Predictability of Seasonal Sahel Rainfall Using GCMs and Lead-Time Improvements Through the Use of a Coupled Model. *Journal of Climate*, *24 (7)*, 1931-1949.

Newell, R. E., and Kidson, J. W. (1984). African mean wind changes between Sahelian wet and dry periods. *International Journal of Climatology*, *4*, 1–7.

Nicholson S. E., Some B., Kone B. (2000). An analysis of recent rainfall conditions in West Africa, including the rainy seasons of the 1997 el Nino and the 1998 la Nina years. *Journal of Climate*, *13(14)*, 2628-2640

Nicholson, S. E. and Grist, J. P. (2001). A conceptual model for understanding rainfall variability in the West African Sahel on interannual and interdecadal timescales. *International Journal of Climatology*, *21*, 1733-1757.

Nicholson, S. E. (1997). An analysis of the ENSO signal in the Tropical Atlantic and western Indian Oceans. *International Journal of Climatology*, *17*, 345-375.

Nicholson, S. E. (2009). A revised picture of the structure of the monsoon and land ITCZ over West African. *Climate Dynamics, 32*, 1155–1171.

Nicholson, S. E., and Grist, J. P. (2003). The seasonal evolution of the atmospheric circulation over West Africa and equatorial Africa. *Journal of Climate, 16*, 1013–1030.

Nicholson, S. E., and Selato, J. C. (2000). The influence of La Niña on African rainfall. *International Journal of Climatology*, *20*, 1761-1776.

North, G. (1975). Theory of energy-balance climate models. *Journal of Atmospheric Sciences, 32*, 2033–2043.

North, G.R. (1984). The small ice cap instability in diffusive climate models. *Journal of Atmospheric Sciences*, *41*, 3390-3395.

Ofori-Sarpong, E. and Annor, J. (2001). Rainfall over Accra, 1901–90. *Weather*, *56*, 55–62.

Oleson, K. W., Niu, G. Y., Yang, Z. L., Lawrence, D. M. and others (2008). Improvements to the Community Land Model and their impact on the hydrologic cycle. *Journal of Geophysical Research, 113*, G01021.

Oleson, K.W., Dai, Y., Bonan, G., Bosilovich, M. and others (2004). Technical description of the Community Land Model. National Center for Atmospheric Research Tech Note NCAR/TN-461+STR, NCAR, Boulder, CO

Omotosho, J. B. (1988). Spatial variation of rainfall in Nigeria during the "little dry season". *Atmospheric Researc*h, *22*, 137–147.

Opoku-Ankomah, Y. and Cordrey, I. (1994). Atlantic Sea Surface Temperatures and Rainfall Variability in Ghana. *Journal of Climate, 7*, 551-558.

Owusu, K. and Waylen, P.R. (2009). Trends in Spatio-Temporal Rainfall Variability in Ghana, (1951-2000). *Weather, 64*, 115-120.

Owusu, K. and Waylen, P.R. (2013). The Changing Rainy Season Climatology of Mid-Ghana. *Theoretical and Applied Climatology, 112*, 419-430.

Pal, J. S., Giorgi, F., Bi, X., Elguindi, N., Solomon, F., Gao, X., Francisco, R., Zakey, A., Winter, J., Ashfaq, M., Syed, F., Bell, J. L., Diffanbaugh, N. S., Kamacharya, J., Konare, A., Martinez, D., da Rocha, R. P., Sloan, L. C. and Steiner, A. (2007). The ICTP RegCM3 and RegCNET: regional climate modeling for the developing world. *Bulletin of American Meteorological Society, 88*, 1395–1409.

Pal, J. S., Small, E. and Eltahir, E. (2000). Simulation of regional-scale water and energy budgets: representation of subgrid cloud and precipitation processes within RegCM. *Journal of Geophysical Research*, *105*, 29579–29594

Patricola, C.M., and Cook, K. H. (2010b). Sub-Saharan Northern African Climate at the end of the twenty-first Century: forcing factors and climate change processes. *Climate Dynamics*. doi:10.1007/s00382-010-0907-y.

Payne, S. W. and McGarry, M. M. (1977). The Relationship of Satellite Inferred Convective Activity to Easterly Waves Over West Africa and the Adjacent Ocean During Phase III of GATE. *Monthly Weather Review*, *105*, 413-420.

Price, C., Yair, Y. and Asfur, M. (2007). East African lightning as a precursor of Atlantic hurricane activity. *Geophysical Research Letter, 34*, L09805, doi: 10.1029/2006GL02888

Qian, J. H. (2008). Why precipitation is mostly concentrated over islands in the maritime continent. Journal of Atmospheric Sciences, *65*, 1428-1441

Qian, J. H., Robertson, A. W. and Moron, V. (2010). Interactions among ENSO, the monsoons, and diurnal cycle in rainfall variability over Java, Indonesia. *Journal of Atmospheric Sciences*, *67*, 3509-3524

Rauscher, S. A., Seth, A., Qian, J. H. and Camargo, S. J. (2006). Domain choice in an experimental nested modeling prediction system for South America. *Theoretical and Applied Climatology*, *86*, 229–246.

Redelsperger, J.-L., and Lafore, J.-P. (1988). A three-dimensional simulation of a tropical squall line: Convection, organization and thermodynamic vertical transport. *Journal of Atmospheric Sciences*, *45*, 1334-1356.

Rodgers, C., van de Giesen, N., Laube, W., Vlek, P.L.G. and Youkhana, E. (2007). The GLOWA Volta Project: A Framework for Water Resources Decision-Making and Scientific Capacity Building in a Transnational West African Basin. *Water Resources Management*, *21*, 295-313.

Rowell, D. P. and Milford, J. R. (1993). On the Generation of African Squall Lines. *Journal of Climate*, *6*, 1181-1193.

Rowell, D. P. (2001). Teleconnections between the tropical Pacific and the Sahel. *Quarterly Journal of the Royal Meteorology Society*, *127*, 1683-1706.

Sathiyamoorthy, V., Pal, P. K. and Joshi, P. C. (2007). Intraseasonal variability of the tropical easterly jet. *Meteorology and Atmospheric Physics*, *96*, 305-316.

Seth, A. and Giorgi, F. (1998). The effects of domain choice on summer precipitation simulation and sensitivity in a regional climate model. *Journal of Climate, 11, no. 10,* 2698– 2712.

Shinoda, M., and Kawamura, R. (1994). Tropical rainbelt, circulation, and sea surface temperatures associated with the Sahelian rainfall trend. *Journal of the Meteorological Society of Japan*, *72*, 341-357.

Solmon, F., Mallet, M., Elguindi, N., Giorgi, F., Zakey, A. and Konaré, A. (2008). Dust aerosol impact on regional precipitation over western Africa, mechanisms and sensitivity to absorption properties. *Geophysical Research Letter*, *35*, L24705, doi: 10.1029/2008GL035900

Steiner, A. L., Pal, J. S., Rauscher, S. A., Bell, J. L. and others (2009). Land surface coupling in regional climate simulations of the West Africa monsoon. *Climate Dynamics*, *33*, 869–892

Sultan, B., and Janicot, S. (2003b). The West African Monsoon Dynamics. Part II: The "Preonset" and "Onset" of the Summer Monsoon. *Journal of Climate, 16*, 3407–3427.

Sultan, B., Baron, C., Dingkuhn, M., Sarr, B. and Janicot, S. (2005). Agricultural Impacts of Large-Scale Variability of the West African Monsoon. *Agricultural and Forest Meteorology*, *128*, 93-110.

Sun, L., Semazzi, F. H. M., Giorgi, F., and Ogallo, L. (1999). Application of the NCAR regional climate model to eastern Africa, 2, Simulation of interannual variability of short rains. *Journal of Geophysical Research, 104*, 6549–6562.

Sylla, M. B., Aquila, A. D., Ruti, P. M. and Giorgi, F. (2010). Simulation of the intraseasonal and the interannual variability of rainfall over West Africa with regCM3 during the monsoon period. *International Journal of Climatology, 30*, 1865–1883.

Sylla, M. B., Coppola, E., Mariotti, L., Giorgi, F., Ruti, P. M., Dell'Aquila, A., and Bi, X. (2009a). Multiyear simulation of the African climate using a regional climate model (RegCM3) with the high resolution ERA Interim reanalysis. *Climate Dynamics*. DOI: 10.1007/s00382-009- 0613-9.

Sylla, M. B., Gaye, A. T., Jenkins, G. S., Pal, J. S. and Giorgi, F. (2010). Consistency of projected drought over the Sahel with changes in the monsoon circulation and extremes in a regional climate model projections. *Journal of Geophysical Research D, 115*, no. 16, Article ID D16108.

Sylla, M. B., Gaye, A. T., Pal, J. S., Jenkins, G. S. and Bi, X. Q. (2009). High resolution simulations of West Africa climate using Regional Climate Model (RegCM3) with different lateral boundary conditions. *Theoretical and Applied Climatology, 98, no. 3-4*, 293–314

Sylla, M. B., Giorgi, F., Ruti, P. M., Calmanti, S., Dell'Aquila, A. (2011).The impact of deep convection on the West African summer monsoon climate:

a regional climate model sensitivity study. *Quarterly Journal of the Royal Meteorology Society, 137*, 1417–1430

Tall, A., Mason, S.J., van Aalst, M., Suarez, P., Ait-Chellouche, Y., Diallo, A.A., Braman, L. (2012). Using Seasonal Climate Forecasts to Guide Disaster Management: The Red Cross Experience during the 2008 West Africa Floods. *International Journal of Geophysics, 2012*, doi: 10.1155 /2012/ 986016.

Tawfik, A. B. and Steiner, A. L. (2011). The role of soil ice in land–atmosphere coupling over the United States: a soil moisture precipitation winter feedback mechanism. *Journal of Geophysical Research, 116*: D02113, doi: 10.1029/2010JD 014333

Thorncroft, C. D, Nguyen, H, Zhang, C. and Peyrillé, P. (2011). Annual cycle of the West African monsoon: regional circulations and associated water vapour transport. *Quarterly Journal of the Royal Meteorology Society, 137*, 129-147.

Thorncroft, C. D. (2001). African easterly wave variability and its relationship to tropical Cyclone activity. *Journal of Climate, 14*, 1166-1179.

Thorncroft, C. D., and Blackburn, M. (1999). Maintenance of the African easterly jet. *Quarterly Journal of the Royal Meteorology Society, 125*, 763-786.

Torma, C., Coppola, E., Giorgi, F., Bartoly, J. and Pongracz, R. (2011): Validation of a high resolution version of the regional climate model RegCM3 over the Carpathian basin. *Journal of Hydrometeorology, 12*, 84–100

Vizy, E. K. and Cook, K. H. (2002). Development and application of a mesoscale climate model for the tropics: influence of sea surface temperature anomalies on the West African monsoon. *Journal of Geophysical Research D, 107,* no. 3, Article ID 4023.

Ward, M. N. (1992). Provisional corrected surface wind data, worldwide ocean-atmosphere surface fields, and Sahelian rainfall variability. *Journal of Climate,* 5, 454–475.

Ward, M. N., Cook, K., Diedhiou, A., Fontaine, B. Giannini, A., Kamga, A., Lamb, P. J., Mohamed, B., Nassor, A., and Thomcroft, C. (2004). Seasonal-to-Decadal Predictability and Prediction of West African Climate. *CLIVAR Exchanges, 9,* 14-20

Ward, M. N., Folland, C. K., Maskell, K., Rowell, D. and Colman, A. (1990). Understanding and predicting seasonal rainfall in sub-Saharan Africa. *WMO Tropical Meteorology Research Programme Report Series, 36,* 157-161.

WMO/TD-No. 876. Proceedings of the first WCRP international conference on reanalysis (*Silver Spring,* Maryland, USA, 27-31 October 1997).

Yang, G. and Slingo, J. (2001). The Diurnal Cycle in the Tropics. *Monthly Weather Review, 129,* 784-801.

Yengoh, G.T. (2010). Trends in Agriculturally-Relevant Rainfall Characteristics for Small-Scale Agriculture in Northern Ghana. *Journal of Agricultural Science, 2,* 3-16.

Zhang, C., Woodworth, P. and Gu, G. (2006). The seasonal cycle in the lower troposphere over West Africa from sounding observations. *Quarterly Journal of the Royal Meteorology Society, 132*, 2559–2582.

Zipser, E. J. (2003). Tropical Precipitating systems. *Handbook of Weather, Climate, and Water: Dynamics, Climate, Physical Weather Systems, and Measurements*, T. Potter and B. Colman, Ed. John Wiley & Sons, New York, Chapter 31.

APPENDICES

A1: Table of Parameters and parameterizations for irrigated agriculture and urban land in four RCMs (From Kueppers et al. (2008))

Table 1
Parameters and parameterizations for irrigated agriculture and urban land represented in the four RCMs

	Irrigated agriculture parameters				Urban parameters			
	RSM	RegCM3	MM5-CLM3	DRCM	RSM	RegCM3	MM5-CLM3	DRCM
Maximum vegetation cover (%)	90	80	85	80	95	5	0	10
Roughness length (m)	0.06	0.06	0.06	0.07	0.2287	1.5	0.01	0.5
Displacement height (m)	N/A	0.0	0.34	N/A	N/A	6.0	N/A	N/A
Minimum stomatal resistance (s/m)	40	45	N/A	36	999	120	N/A	999
Maximum leaf area index	N/A	6	6	4	N/A	1	N/A	4
Top soil layer depth (cm)	10	10	1.75	7	10	10	1.75	7
Total soil depth (m)	2	3	3.4	2.55	2	3	3.4	2.55
Soil texture type (sand/silt/clay, %)	Sandy loam (58:32:10)[a]	Loam (43:39:18)	Sandy clay loam (58:15:27)[a]	Multiple	Loamy sand (82:12:6)[a]	Clay (22:20:58)	Sand (92:5:3)[a]	Multiple
Vegetation albedo[b]	VIS: 0.10 NIR: 0.30	VIS: 0.08 NIR: 0.28	VIS: 0.11 NIR: 0.58	Total: 0.15–0.19	VIS: 0.09 NIR: 0.29	VIS: 0.02 NIR: 0.15	N/A	Total: 0.15
Soil moisture modification	Saturation (all time steps)	Field capacity (all time steps)	None	4.8225×10^{-8} m s^{-1}[c]	None	None	None	Fixed at 0.05 kg/kg

[a] Soil types are parameterized separately from vegetation types; values given are the dominant values for the urban and agricultural grid cells in the MOD case.
[b] VIS is for the visible range (0.4–0.7 nm); NIR is for the near-infrared range (>0.7 nm).
[c] 4.8225×10^{-8} m s^{-1} when the top soil layer temperature is greater than 12 °C, and zero when less than 12 °C.

A2: Ferret codes in plotting linear association between SSTs and Rainfall over West Africa

use tsaindex.nc

use gpcpjja.nc

use TRMMjja.mon.1998-2009.nc

use eraintjja.nc

use regcm4jja.nc ! change this to your data

ppl tics .1,.1,.1,-1,-1

! go multi_view [rows],[columns], [xsize],[xstart],[xgap], [ysize],[ystart],[ygap],[prefix]

go multi_view 2, 2, 0.18, 0.1, 0.05, 0.16, 0.11, 0.07

let sea=8

let ssn = `sea`

!set window/aspect=0.5 !change this to suit yours

set view UL

let pp = pr[d=2] !Change only pre to your variable

let regidx = index[d=1,gt=pp@ave]

let sspre = (pp[l=@SHF:-2] + pp[l=@SHF:-1] + pp[l=@SHF:0])/3 ! this will give you JJA -- same as below

let ssidx = (regidx[l=@SHF:-2] + regidx[l=@SHF:-1] + regidx[l=@SHF:0])/3

let p=sspre[d=2,l=`ssn`:228:12] ! this define the length of time . It should be same for p and q

let q=ssidx[d=1,l=`ssn`:228:12]

go variance

fill /nolab/level=(-inf)(-0.9,0.9,0.2)(inf)/pal=orange_purple correl[y=0:25,x=-20:20]; go land 7 "" 1 ! change your x and y to your domain

label -26, 26,-20,0,0.15, @SR@P1 (a) Correlation between TSA SST and GPCP JJA rainfall

! Repeat for other 3 dataset like this

set view UR

let pp = hrf[d=3] !Change only pre to your variable

let regidx = index[d=1,gt=pp@ave]

let sspre = (pp[l=@SHF:-2] + pp[l=@SHF:-1] + pp[l=@SHF:0])/3 ! this will give you JJA -- same as below

let ssidx = (regidx[l=@SHF:-2] + regidx[l=@SHF:-1] + regidx[l=@SHF:0])/3

let p=sspre[d=3,l=`ssn`:228:12] ! this define the length of time . It should be same for p and q

let q=ssidx[d=1,l=`ssn`:228:12]

go variance

fill /nolab/level=(-inf)(-0.9,0.9,0.2)(inf)/pal=orange_purple correl[y=0:25,x=-20:20]; go land 7 "" 1 ! change your x and y to your domain

label -26, 26,-20,0,0.15, @SR@P1 (b) Correlation between TSA SST and TRMM JJA rainfall

set view LL

let pp = pr[d=4] !Change only pre to your variable

let regidx = index[d=1,gt=pp@ave]

let sspre = (pp[l=@SHF:-2] + pp[l=@SHF:-1] + pp[l=@SHF:0])/3 ! this will give you JJA -- same as below

let ssidx = (regidx[l=@SHF:-2] + regidx[l=@SHF:-1] + regidx[l=@SHF:0])/3

let p=sspre[d=4,l=`ssn`:228:12] ! this define the length of time . It should be same for p and q

let q=ssidx[d=1,l=`ssn`:228:12]

go variance

fill /nolab/level=(-inf)(-0.9,0.9,0.2)(inf)/pal=orange_purple correl[y=0:25,x=-20:20]; go land 7 "" 1 ! change your x and y to your domain

label -26, 26,-20,0,0.15, @SR@P1 (c) Correlation between TSA SST and ERAINT JJA rainfall

set view LR

let pp = tpr[d=5] !Change only pre to your variable

let regidx = index[d=1,gt=pp@ave]

let sspre = (pp[l=@SHF:-2] + pp[l=@SHF:-1] + pp[l=@SHF:0])/3 ! this will give you JJA -- same as below

let ssidx = (regidx[l=@SHF:-2] + regidx[l=@SHF:-1] + regidx[l=@SHF:0])/3

let p=sspre[d=5,l=`ssn`:228:12] ! this define the length of time . It should be same for p and q

let q=ssidx[d=1,l=`ssn`:228:12]

go variance

fill /nolab/level=(-inf)(-0.9,0.9,0.2)(inf)/pal=orange_purple correl[y=0:25,x=-20:20]; go land 7 "" 1 ! change your x and y to your domain

label -27, 26,-20,0,0.15, @SR@P1 (d) Correlation between TSA SST and REGCM4 JJA rainfall

FRAME/FILE=correlationjja.gif